INVESTIGATING THE RELATIONSHIP BETWEEN INVASIVE CARDIAC OUTPUT MEASUREMENTS AND CEREBRAL BLOOD VELOCITY DURING THE ACTIVE STAND TEST IN HEALTHY ADULTS

PALINA BURNEIKO

A THESIS SUBMITTED TO THE FACULTY OF GRADUATE STUDIES IN PARTIAL FULFILLMENT OF THE REQUIREMENTS FOR THE DEGREE OF MASTER OF SCIENCE

GRADUATE PROGRAM IN KINESIOLOGY AND HEALTH SCIENCE

YORK UNIVERSITY

TORONTO, ONTARIO

August 2026

© Palina Burneiko, 2026

Abstract

This study investigated the association between changes in cardiac output (CO) and alterations in cerebral blood velocity (CBV) in healthy adults during standing. Participants completed two visits of active standing (5-min supine, 10-min standing). Visit one included continuous blood pressure (BP), heart rate (HR), and middle cerebral artery blood velocity. During Visit 2, right heart catheterization was performed to measure right atrial, ventricular, pulmonary and pulmonary capillary wedge pressures. Thermodilution derived CO was obtained. Venous and arterial oxygenation, HR and BP were concurrently measured. Static and dynamic cerebral autoregulation were analyzed. Changes in mean CBV were positively correlated with systolic and diastolic CBV and negatively associated with cerebrovascular resistance index. Changes in mean CBV were positively correlated with changes in autoregulatory high frequency phase and negatively correlated with changes in right ventricular systolic pressure, pulmonary artery wedge pressure, and absolute oxygen consumption with no effect of changing CO during standing.

Acknowledgements

I would like to begin by expressing my sincere gratitude to my supervisor, Dr. Heather Edgell, for her exceptional guidance, mentorship, and unwavering support throughout my graduate studies. Thank you for sharing your knowledge and expertise, for continually encouraging me to think critically, and for challenging me to grow as a researcher. Your patience, confidence in my abilities, and dedication to my success have been invaluable, and I am truly grateful for the opportunity to have learned from you.

I would also like to extend my sincere thanks to Dr. Susanna Mak and the entire staff of the Clinical Cardiovascular Catheterization Research Laboratory at Mount Sinai Hospital. This research would not have been possible without your generosity, expertise, and willingness to support this project. Thank you to the nurses and administrative staff for your professionalism and kindness, and for ensuring that every study visit ran smoothly. I am also incredibly grateful to the graduate students Maya, Karlo, and Josh for their assistance with data collection, their teamwork, and for making long days in the lab both productive and enjoyable.

To my lab mates—Olivia, Liv, Rafia, and Veronica—thank you for creating such a welcoming, supportive, and collaborative environment. I am grateful for your encouragement, willingness to help, and the countless conversations, laughs, and shared experiences that made my time in the lab so memorable. I have truly enjoyed working alongside each of you.

Finally, I would like to thank my family and loved ones for their endless love and support. To my mama, Zhanna, and my sister, Nadya, thank you for always believing in me, encouraging me through every challenge, and celebrating every milestone along the way. Your support has meant more than words can express. To my boyfriend, Tim, thank you for your patience, encouragement, and constant reassurance throughout this journey. Thank you for always being there to celebrate the successes, help me through the setbacks, and remind me to keep going. I could not have accomplished this without all of you.

Table of Contents

Abstract ii

Acknowledgements iii

Table of Contents iv

List of Tables vii

List of Figures viii

List of Abbreviations ix

Chapter 1: Literature Review 1

1.1 General Introduction 1

1.2 Understanding Vascular Regulation 1

1.2.1 Cardiovascular System 1

1.2.2 Autonomic Nervous System 3

1.3 Measurements of Cardiovascular Function 5

1.3.1 Thermodilution 5

1.3.2 Direct Fick 5

1.3.3 Active Stand Test 6

1.4 Cerebral Blood Flow 7

1.4.1 Cerebrovascular System Anatomy 7

1.4.2 Orthostasis & Cerebral Blood Flow 8

1.4.3 Cerebral Autoregulation 9

1.5 Measurements of Cerebral Flow 10

1.6 Research Objectives 11

1.7 Hypotheses 11

Chapter 2: Materials and Methods 13

2.1 Participants 13

2.2 Study Design 13

2.3 Visit 1 Protocol 14

2.3.1 Hemodynamic Measurements 15

2.3.2 Indices of Cerebral Blood Flow 15

2.3.3 Heart Rate Variability 16

2.3.4 Cardiovagal Baroreceptor Sensitivity 17

2.3.5 Data Acquisition 17
2.4 Visit 2 Protocol 17
2.4.1 Right Heart Catheterization Procedure 18
2.4.2 Cardiac Output Measurements 22
2.4.3 Hemodynamic Measurements & Peripheral Muscle Oxygen Saturation 23
2.4.4 Data Acquisition 24
2.5 Data and Statistical Analysis 24

Chapter 3: Results 26
3.1 Non-Invasive Active Stand Results (Visit 1) 26
3.1.1 Hemodynamics 27
3.1.2 Cerebrovascular Responses 27
3.1.3 Cerebral Static Autoregulation 28
3.1.4 Cerebral Dynamic Autoregulation 31
3.1.5 Cardiac Autonomic Function Measures 34
3.1.6 Comparisons of the Change of Mean Cerebral Blood Velocity to the Changes of Hemodynamic, Cerebrovascular, and Autonomic Variables with Standing 37
3.2 Invasive Active Stand Results (Visit 2) 45
3.2.1 Hemodynamics 47
3.2.2 Cardiac Output Measurements 47
3.2.3 Pulmonary Blood Pressures 47
3.2.4 Blood Oximetry 48
3.2.5 Peripheral Muscle Oxygenation 49
3.2.6 Ventilation & Oxygen Consumption 49
3.2.7 Comparison of the Change of Mean Cerebral Blood Velocity to the Changes of Cardiopulmonary Hemodynamic Measurements 53

Chapter 4: Discussion 59
4.1 Summary 59
4.2 Associations Between Changes in Cardiac Output and Cerebral Blood Velocity During Orthostasis 60
4.3 Associations Between Changes in Cardiac Measures and Cerebral Blood Velocity During Orthostasis 60
4.4 Associations Between Changes in Autonomic Function and Cerebral Blood Velocity During Orthostasis 61

4.5 Associations Between Changes in Cerebral Autoregulation and Cerebral Blood Velocity During Orthostasis 62

4.6 Associations Between Changes in Ventilation and Cerebral Blood Velocity During Orthostasis 64

4.7 Limitations and Future Directions 64

4.8 Conclusions 67

References 69

List of Tables

Table 1. Participant baseline characteristics on non-invasive testing day 26

Table 2. Hemodynamic and cerebrovascular responses to the non-invasive active stand test 29

Table 3. Spectral and transfer function analysis of blood pressure and MCAv during the non-invasive active stand test 32

Table 4. HRV during the non-invasive active stand test (n=16) 35

Table 5. Cardiovagal baroreceptor sensitivity (cBRS) during the non-invasive active stand test (n=16) 36

Table 6. Linear regression analysis of mean MCAv and hemodynamic, cerebrovascular, and autonomic measures during the non-invasive active stand test 38

Table 7. Participant baseline characteristics on the invasive testing day 45

Table 8. Cardiopulmonary hemodynamic responses to the invasive active stand test (n=14) 50

Table 9. Linear regression analysis of the change in mean MCAv vs the changes in cardiopulmonary hemodynamic measures during the invasive active stand test 54

List of Figures

Figure 1. A pulmonary artery catheter with the associated transducers 19

Figure 2. Intracardiac locations of pulmonary catheter transducers 20

Figure 3. Placement of the arm during Visit 2 21

Figure 4. An example of a thermodilution temperature-time curve used to derive CO. 22

Figure 5. Association between changes in systolic middle cerebral artery velocity (MCAv) and mean MCAv due to standing. 41

Figure 6. Association between changes in diastolic middle cerebral artery velocity (MCAv) and mean MCAv due to standing. 42

Figure 7. Association between changes in cerebrovascular resistance index (CVRi) and mean middle cerebral artery velocity (MCAv) due to standing 43

Figure 8. Association between changes in high frequency (HF) phase and mean middle cerebral artery velocity (MCAv) due to standing. 44

Figure 9. Association between changes in right ventricular systolic pressure (RVSP) and mean middle cerebral artery velocity (MCAv) due to standing. 56

Figure 10. Association between changes in pulmonary artery wedge pressure (PAWP) and mean middle cerebral artery velocity (MCAv) due to standing. 57

Figure 11. Association between changes in absolute oxygen uptake (VO_2) and mean middle cerebral artery velocity (MCAv) due to standing. 58

List of Abbreviations

ACA: Anterior cerebral artery

ANS: Autonomic nervous system

AST: Active stand test

au: Arbitrary units

BMI: Body mass index

BSA: Body surface area

BP: Blood pressure

BRS: Cardiovascular baroreceptor sensitivity

CaO_2: Arterial oxygen content

CBF: Cerebral blood flow

cBRS: Cardiovagal baroreflex sensitivity

CO: Cardiac output

CO_{DF}: Direct Fick cardiac output

CO_{TD}: Thermodilution cardiac output

CoW: Circle of Willis

CPBR: Cardiopulmonary baroreceptors

CPP: Cerebral perfusion pressure

CrCP: Critical closing pressure

CVR: Cerebrovascular resistance

CVRi: Cerebrovascular resistance index

CvO_2: Mixed-venous oxygen content

DBP: Diastolic blood pressure

HF: High frequency

HHb: Relative deoxyhemoglobin

HR: Heart rate

HRV: Heart rate variability

LF: Low frequency

LF/HF: Ratio of low- to high-frequency components of heart rate variability

MAP: Mean arterial blood pressure

MCA: Middle cerebral artery

MCAv: Middle cerebral artery velocity

mPAP: Mean pulmonary artery pressure

MRI: Magnetic resonance imaging

nGain: Normalized gain

NIRS: Near-infrared spectroscopy

NN50: Absolute number of NN intervals >50 ms

nu: Normalized units

OH: Orthostatic hypotension

OI: Orthostatic intolerance

O_2Hb: Relative oxyhemoglobin

PA: Pulmonary artery

PAWP: Pulmonary artery wedge pressure

PCA: Posterior cerebral artery

PI: Pulsatility index

PNS: Parasympathetic nervous system

pNN50: Percentage of NN intervals greater than 50 ms

POTS: Postural orthostatic tachycardia syndrome

RA: Right atrium

RaP: Right atrial pressure

RAP: Resistance area product

RI: Resistance index

RMSSD: Root mean square of successive differences between RR intervals

Rf: Respiratory frequency

RV: Right ventricle

RVDP: Right ventricular diastolic pressure

RVEDP: Right ventricular end-diastolic pressure

RVSP: Right ventricular systolic pressure

SaO_2: Arterial oxygen saturation

SBP: Systolic blood pressure

SD1: Standard deviation of short-term NN interval variability

SD2: Standard deviation of long-term NN interval variability

SDRR: Standard deviation of all RR intervals

SmO_2: Vastus lateralis muscle oxygenation

SNS: Sympathetic nervous system

SV: Stroke volume

SvO_2: Mixed-venous oxygen saturation

SV_{DF}: Direct Fick stroke volume

SV_{TD}: Thermodilution stroke volume

TCD: Transcranial Doppler

THb: Relative total hemoglobin

Tv: Tidal volume

V_E: Minute ventilation

V_Ei: Minute ventilation indexed to BSA

VO_2: Oxygen uptake

VR: Venous return

VLF: Very low frequency

Chapter 1: Literature Review

1.1 General Introduction

The hemodynamic response to postural change is a physiological stressor to the body. During upright posture (orthostasis), the body depends on rapid cardiovascular and autonomic adjustments to maintain adequate blood flow to meet metabolic demands. The hemodynamic response to standing is readily assessed through measurements of blood pressure (BP) and heart rate (HR) (reviewed in Stewart, 2013) and can be indicative of autonomic dysfunction. Orthostatic intolerance (OI) is defined by the onset of symptoms upon standing that are alleviated with a return to a supine position (Robertson, 1999). Common orthostatic symptoms include; dizziness, light-headedness, fatigue, cognitive difficulties, blurred vision, and tremulousness (Low et al., 1995). OI conditions, such as postural orthostatic tachycardia syndrome (POTS) and orthostatic hypotension (OH), can impair daily function by increasing the risk of falling and reducing quality of life, with a higher prevalence in women than men (Convertino, 1998). OH is defined as a drop of at least 20 mmHg in systolic blood pressure (SBP) or 10 mmHg in diastolic blood pressure (DBP) during the initial 3 minutes of standing up or during tilt table testing (Freeman et al., 2011). POTS is defined as a sustained increase in HR of at least 30 beats per minute or as a HR of more than 120 beats per minute within 10 minutes of standing up or during tilt table testing (reviewed in Stewart, 2013).

1.2 Understanding Vascular Regulation

1.2.1 Cardiovascular System

The cardiovascular system delivers blood supply throughout the body and is comprised of the heart, arteries, veins, and capillaries. Cardiovascular regulation is influenced by multiple factors (i.e. changes in blood volume, medications, hormonal and electrolyte status, osmolarity, and inputs from the adrenal glands and kidneys) and responds to inputs from the autonomic nervous system (ANS) (reviewed in Donald & Shepherd, 1980).

Hemodynamics refers to the physical principles governing blood flow through the cardiovascular system. These principles are fundamentally described by Ohm's law, which relates the current (I) to the voltage gradient (V) and resistance (R) by $R= V/I$. In the context of blood flow, electrical current is analogous to blood flow, the voltage difference corresponds to

the pressure gradient, and the electrical resistance represents vascular resistance (reviewed in Secomb, 2016). Hence, blood flow is determined by the pressure gradient across a vascular bed relative to its resistance (Eq. 1).

$$Flow = \frac{\Delta P}{R} = \frac{arterial\ pressure - venous\ pressure}{R} \quad \text{(Eq. 1)}$$

ΔP is the pressure difference between two points along a length of a blood vessel. R is the resistance to flow.

At the systemic level, blood flow can be described using the relationship between flow, pressure, and resistance, where CO represents total systemic blood flow. Similar to Ohm's law, CO is determined by the pressure gradient between mean arterial pressure (MAP) and central venous pressure, divided by systemic vascular resistance, which is also referred to as total peripheral resistance (Eq. 2) (Levy, 1979). Blood flows down a pressure gradient from areas of high pressure to areas of low pressure. Thus, within systemic circulation, blood flows from high pressure arterial circulation towards lower-pressure venous circulation, with the pressure gradient being generated due to the pumping action of the heart (reviewed in Secomb, 2016).

$$CO = \frac{(MAP - CVP)}{SVR} \quad \text{(Eq. 2)}$$

CO is cardiac output, *CVP* is central venous pressure, *MAP* is mean arterial pressure, *SVR* is systemic vascular resistance.

In the context of blood flow across a vascular bed or an organ, the pressure gradient/difference is determined by the difference between arterial pressure and venous pressure, such that flow is dependent on the driving pressure across the organ and the resistance imposed by its vasculature (reviewed in Goodwill et al., 2017). Additionally, differences in

metabolic demand among organs contribute to differences in regional blood flow. At the regional level, blood velocity is directly proportional to blood flow which is depicted as a product of velocity (speed of blood movement) and the cross-sectional area of the vessel (reviewed in Dremin et al., 2025), where increases in cross-sectional area are associated with decreases in blood velocity (Eq. 3).

$$Perfusion\ Pressure = Arterial\ Pressure - Venous\ Pressure = (v\ x\ A)(R)$$

A is cross sectional area of a vessel, *v* is blood velocity, *R* is the resistance to flow. (Eq. 3)

When supine, about 30% of circulatory blood is in the thoracic cavity (Thompson et al., 1928). When transitioning to an upright posture from a supine posture, the effect of gravity will result in a displacement of 300 - 800 mL of blood from the upper body to the lower extremities (reviewed in Grubb et al., 2008), resulting in pooling of blood. The hydrostatic pressure gradient is further increased within the capillary network as a result of a plasma volume shift of 10% from the intravascular space to the interstitial spaces of the lower extremities (Jacob et al., 1998). This drop in central blood volume, along with the gravitational pooling of blood and plasma in the lower body, will cause reductions in venous return (VR), stroke volume (SV), BP, cardiac output (CO), and cerebral blood flow (CBF). Normally, the body will engage multiple regulatory mechanisms to compensate for venous pooling and the hemodynamic changes to maintain BP and ensure sufficient tissue perfusion.

1.2.2 Autonomic Nervous System

The interaction between the sympathetic nervous system (SNS) and parasympathetic nervous system (PNS) is important for supporting the physiological demands of the body during orthostatic stress through modifications to HR and BP. The SNS regulates cardiovascular function primarily through the release of norepinephrine (Euler, 1948) and cotransmitters such as neuropeptide Y and adenosine-triphosphate (Macarthur et al., 2011), which induce arterial and venous constriction, augment cardiac contractility, and increase HR. The PNS acts through vagal

efferent fibres and influences HR, particularly at rates less than the intrinsic rate (Raczak et al., 1999). The intrinsic rate is the rate of the sinoatrial node of the heart without any influence from the ANS, approximately 100 beats per minute (reviewed in Gordan et al., 2015). Importantly, the cardiovascular system contains arterial (carotid sinus and aortic arch) and cardiopulmonary baroreceptors (CPBR), which are specialized mechanoreceptors that are responsive to BP changes in the body (Korner, 1971).

At rest or when supine, these baroreceptors exert a tonic inhibitory influence on cardiovascular control centres in the medulla, particularly the nucleus tractus solitarius, reducing SNS output. Neuronal input from stretching these receptors enhances activity in the dorsal motor nucleus of the vagus and nucleus ambiguus and concurrently suppresses sympathoexcitatory neurons in the rostral ventrolateral medulla (reviewed in Grubb et al., 2008). While standing, decreases in VR, cardiac filling pressures, and BP result in reduced stretch of the baroreceptors. Subsequently, the baroreceptor firing rates to the medulla oblongata decline, which result in an increase of sympathetic output (reviewed in Grubb et al., 2008) and parasympathetic withdrawal to increase HR and BP. In healthy individuals, baroreflex mechanisms (arterial and cardiopulmonary) can elicit rapid HR increases within 1-3 seconds, peripheral arterial and venous vasoconstriction within 10-30 seconds, and cardiac contractility within 3-8 seconds (reviewed in Finucane et al., 2019). Therefore, the baroreflex can correct BP within approximately 30-40 seconds (Kaufmann et al., 2020) after standing. However, in those people who suffer from OI, disrupted autonomic regulation impairs the function of these compensatory responses.

Abnormal autonomic regulation can include baroreflex dysfunction, which involves changes in afferent baroreflex engagement and sensitivity (reviewed in Freeman et al., 2018). Decreased sensitivity impairs the ability of baroreceptors to detect both increases and decreases in BP (Robertson et al., 1993), resulting in insufficient parasympathetic and sympathetic responsiveness. In the case of certain types of OH (i.e. neurogenic), insufficient parasympathetic withdrawal may hinder the increase in HR necessary to maintain adequate CO (reviewed in Benarroch, 2008). Further, in these individuals with OH, impaired sympathetic regulation may lead to reduced peripheral vasoconstriction, exacerbating venous pooling and thus reducing VR to the heart.

1.3 Measurements of Cardiovascular Function

1.3.1 Thermodilution

Thermodilution is a widely employed technique used to accurately measure CO and intracardiac pressures in a clinical setting. This technique gained popularity with the invention of the pulmonary artery (PA) catheter by Swan and Ganz and the development of analogue computers for CO calculations (reviewed in Argueta & Paniagua, 2019). The thermodilution method utilizes a flow-directed balloon-tipped catheter, which allows reliable and accurate passage to the PA (Forrester et al., 1972). Thermodilution CO is typically measured via a protocol where a known volume of cold saline is injected into the right atrium (RA) of the heart, and the blood temperature changes are detected downstream in the PA by a temperature sensor (i.e. thermistor) (described in detail in the Methods). Forrester and colleagues (1972) described that the rate of temperature recovery is inversely proportional to CO, with a faster recovery of cooled blood to that of body temperature indicating higher flow. CO is then derived using the Stewart-Hamilton equation (described in Methods) that depicts the relationship between blood flow, the saline indicator, and blood concentration (reviewed in Argueta & Paniagua, 2019).

PA thermodilution is frequently reviewed as a "gold standard" in method comparison studies (Rajaram et al., 2013) and remains the preferred method for CO monitoring in a clinical setting (reviewed in Kouz et al., 2021). However, several factors may contribute to potential errors when obtaining the CO measurement. Rapid infusions of saline indicator (Wetzel & Latson, 1985), poor timing with the respiratory cycle (Stevens et al., 1985), extremely low CO (van Grondelle et al., 1983), and inaccurate thermistor placement can overestimate or underestimate measurements obtained. The requirement for invasive instrumentation and trained healthcare professionals in a clinical setting contributes to the procedural complexity of this technique.

1.3.2 Direct Fick

The direct Fick method of determining CO is another invasive method that was described by Adolph Fick in 1870 (reviewed in Geerts et al., 2011). This method requires two components: a PA catheter measuring filling pressures and a metabolic analyzer to record oxygen consumption (Schurr & Genuardi, 2024) (described in detail in the Methods). The basic principle

of this method proposes that pulmonary oxygen uptake is fully transferred to the blood, such that total oxygen exchange across the lungs is equal to the product of pulmonary blood flow and the difference between arterio-venous oxygen content (Mathews & Singh, 2008). Studies have demonstrated comparable results between Fick and thermodilution techniques for CO reporting a highly significant correlation between the two (Branthwaite & Bradley, 1968; Kubo et al., 1987). These previous studies focused on populations with various cardiovascular diseases (i.e. congestive heart failure, systemic hypertension) and patients who required right heart catheterization for treatment or diagnosis, rather than in health.

1.3.3 Active Stand Test

The active stand test (AST) is widely utilized for the evaluation of OI syndromes. This non-invasive procedure assesses HR and BP responses during the transition from supine rest to unsupported standing, thereby reproducing the physiological stressors that typically elicit symptoms in individuals with OI. The AST can be conducted in both clinical and community settings. In clinical settings, the use of beat-to-beat BP and HR monitoring enables identification of transient hemodynamic responses that conventional intermittent BP measurements may miss (reviewed in Breslin et al., 2023). The AST is composed of two sequential components: the supine rest phase and the unsupported upright standing phase. Clinicians and researchers observe BP and HR responses during the transition between postures and for a pre-determined period of standing (3-10 minutes, depending on the protocol).

During the supine phase, the patient is asked to lie for 5-10 minutes, allowing for adequate cardiovascular stabilization (Frith et al., 2013). A 5-minute rest period is sufficient to establish stable baseline BP values. Mader et al. found that shorter durations (< 5 minutes) may result in unstable baselines, whereas prolonged rest periods (> 10 minutes) can exaggerate the initial BP decline upon standing (Mader et al., 1989). The resting phase allows for detection of supine hypertension and acquisition of HR and BP variability, which are indicators of autonomic balance (reviewed in Finucane et al., 2019). Spontaneous baroreflex sensitivity (often referred to as cardiovagal) can also be quantified from these data (Westerhof et al., 2004), providing insight into the integrity of short-term baroreflex-mediated HR control (reviewed in Finucane et al., 2019). Following the supine phase, individuals are asked to stand up and remain standing for 3-

10 minutes (Breslin et al., 2023; Edgell et al., 2012; reviewed in Finucane et al., 2019; Hernández et al., 2024; Tse et al., 2005).

1.4 Cerebral Blood Flow

1.4.1 Cerebrovascular System Anatomy

The brain is a highly metabolically demanding organ in the human body and relies on a highly regulated cerebrovascular network to preserve adequate CBF (Peters et al., 2004). This system ensures continuous delivery of essential substrates (i.e. glucose and oxygen) that are essential to maintain cognitive function and support neural activity (Chandra et al., 2017). The cerebral arterial system can be divided into two primary circulations: anterior and posterior. The anterior circulation is composed of the internal carotid arteries, middle cerebral arteries (MCA), anterior cerebral arteries (ACA), and the anterior communicating artery (reviewed in Deshpande et al., 2025). The posterior circulation includes the vertebral arteries, basilar artery, and the posterior cerebral arteries (PCA) (reviewed in Chandra et al., 2017). The anterior circulation primarily supplies blood to the majority of the forebrain, including the temporal, parietal, and frontal lobes, as well as portions of the diencephalon and internal capsule (Zarrinkoob et al., 2015). The posterior circulation supplies blood to the occipital lobe, cerebellum, and the posterior portions of the brainstem (Hussein et al., 1988). The anterior and the posterior circulation systems are interconnected through the posterior communicating arteries, forming the Circle of Willis (CoW) (reviewed in Deshpande et al., 2025). The CoW is located at the base of the brain, creating a ring of arteries around the optic chiasm and the pituitary gland (reviewed in Chandra et al., 2017; Patel et al., 2024). Notably, the branching patterns within the CoW help modulate intracranial pressure and blood flow fluctuations, contributing to microvascular stability (reviewed in Vrselja et al., 2014). Postural studies typically examine the MCA and/or the PCA as indices of CBF, largely due to the accessible signals from these vessels (Clough et al., 2024; Sorond et al., 2005; Zhong et al., 2025). Across all the arteries in the brain, the MCA is the largest, and thus easiest to access with ultrasound (Chandra et al., 2017; Patel et al., 2024), and perfuses the majority of the lateral cerebral hemispheres.

As with systemic arteries, cerebral arteries are made up of 3 layers: tunica intima, tunica media, and tunica adventitia (Milutinović et al., 2020); however, cerebral arteries differ structurally. Cerebral arteries contain limited elastin fibres within the medial layer and thin

adventitia, lack an external elastic lamina (i.e. located between the medial and adventitia layers), but have a well-developed internal elastic lamina (i.e. located between intimal and medial layers) (reviewed in Vrselja et al., 2014). These structural properties lead to reduced elasticity, increased susceptibility to mechanical stress, and a reliance on active vasoregulation to maintain stable CBF.

1.4.2 Orthostasis & Cerebral Blood Flow

Cerebral blood flow is governed by the same fundamental principles of pressure-driven flow described by Ohm's law, whereby flow is proportional to the pressure gradient across the vascular bed and inversely proportional to vascular resistance. In the cerebral circulation, the pressure difference or the driving pressure is represented by cerebral perfusion pressure (CPP). CPP is defined as the difference between mean arterial pressure (MAP) and the intracranial pressure, which reflects the pressure of the cerebrospinal fluid in the subarachnoid space (reviewed in Fantini et al., 2016). Under normal supine conditions, intracranial pressure is relatively low (between 7-15 mmHg) and cerebral venous pressure is typically 2-5 mmHg (reviewed in Fantini et al., 2016; reviewed in Munakomi & Das, 2026). During upright posture, gravity pulls venous blood towards the heart and promotes venous pooling in areas below the level of the heart, resulting in marked reductions in venous pressure at the level of cerebral circulation (Olufsen et al., 2005). Consequently, the cerebral venous pressure approaches zero, such that the effective cerebral perfusion pressure gradient is determined primarily by the arterial pressure, therefore driving the movement of blood, a phenomenon referred to as the "waterfall effect" (reviewed in Castro et al., 2026). Thus, cerebral perfusion pressure can be approximated as (arterial pressure – venous pressure)=MAP when central venous pressure approaches zero (reviewed in Mount & Das, 2026). This supports the use of MAP as the primary determinant of CPP (reviewed in Fantini et al., 2016; Vedantam et al., 2019) in the present study, as incorporating a venous pressure term would have little influence when cerebral venous pressure is negligible.

As described above, upon orthostasis, gravity pulls blood into the lower body, which reduces the amount of blood returning to the heart, leading to drops in CO and therefore CBF in healthy humans (reviewed in Khan et al., 2025). Indeed, Edgell et al. demonstrated that both CBF and CO were reduced with orthostatic stress when evaluating blood velocity changes in the

MCA (Edgell et al., 2012). However, a causal link between the two was not made. Various factors can affect CBF along with CO, including CPP and cerebrovascular resistance (CVR). CPP is defined as the pressure gradient at the hydrostatic level of the brain that drives CBF (reviewed in Khan et al., 2025). When supine, BP is equal in the brain and the body. In upright posture, there is a reduction in BP in the brain (Rosner & Coley, 1986; Schwarz et al., 2002) due to the hydrostatic gradient that is created by gravity. This introduces a pressure gradient between the head and the lower body, where arterial BP is lowest at the head and greatest in the feet (Favre et al., 2020; reviewed in Hinghofer-Szalkay, 2011). To preserve CBF while CPP is lower when upright, cerebral vessels must vasodilate (Hinghofer-Szalkay, 2011). CVR reflects the resistance to blood flow within the cerebral vasculature, and is primarily regulated through changes in vessel diameters (reviewed in Khan et al., 2025). Therefore, increases in CVR reduce CBF, and decreases in CVR increase CBF.

1.4.3 Cerebral Autoregulation

The brain contains an intrinsic homeostatic mechanism that adjusts the tone of cerebral vessels to maintain sufficient CBF. Cerebral autoregulation is the process by which cerebrovasculature adjusts to a wide variation of perfusion pressure to maintain stable blood flow in order to prevent damage to the vessels, support the brain's continuous metabolic demands and manage waste production (Lassen & Christensen, 1976). There are four mechanisms through which CBF is regulated via changing vasomotor tone; activation of autonomic neural pathways, accumulation of metabolic by-products (arterial O_2 and CO_2, H+, etc.), myogenic response to changing pressure, and the response to vasoactive substances (i.e. nitric oxide) (Armstead, 2016; Mchedlishvili, 1980). However, in individuals who suffer from OI, impairments of these mechanisms could contribute to insufficient CBF control.

Cerebral autoregulation can be assessed using static or dynamic approaches. Static indices of autoregulation examine changes in perfusion pressure and CBF over an extended period of time, while dynamic cerebral autoregulation assesses the immediate vascular responses to pressure fluctuations (Aaslid et al., 1989). Static measurements assess the overall effectiveness of autoregulation but do not provide information on the timeframe in which the changes in CVR are achieved (Tiecks et al., 1995) nor the sensitivity of the relationship between changes in BP and CBF. In contrast, dynamic measurements capture both the magnitude, timing, and sensitivity

of the vascular response to changing BP. A study conducted by Tiecks et al. indicated that static and dynamic assessments of autoregulation yielded comparable results in normal adults with impaired or intact autoregulation, demonstrating a good correlation between both methods (Tiecks et al., 1995).

1.5 Measurements of Cerebral Flow

Transcranial Doppler (TCD) ultrasound is a common non-invasive technique that is used as an index of CBF by measuring blood velocity change in a cerebral artery (reviewed in Khan et al., 2025). Measuring blood velocity in the brain does not equate to flow as the size of the artery is unknown. Therefore, to assume that TCD measurements are representative of total CBF, three assumptions must be met: (1) the diameter of the insonated blood vessel does not change, (2) the insonation angle remains fixed in place, and (3) changes in blood flow through one MCA is representative of all of the cerebral arteries (e.g. MCA, ACA, and PCA) (reviewed in Khan et al., 2025).

Valdueza et al. examined the effects of hyperventilation (i.e. hypocapnic condition) on MCA diameter and velocity, using magnetic resonance imaging (MRI) and TCD, respectively (Valdueza et al., 1997). During hyperventilation, they reported no significant changes to MCA diameter. Serrador et al. similarly examined the effects of orthostatic stress (also a hypocapnic condition) on MCA diameter and velocity, using MRI and TCD ultrasound (Serrador et al., 2000), and reported that under orthostatic conditions, no changes in MCA diameter were detected (Serrador et al., 2000). Thus, we assume that the artery size does not change during upright posture; however, it should be noted that Valdueza et al. (1997) used hyperventilation and Serrador et al. (2000) used lower body negative pressure rather than upright posture.

Studies using TCD ultrasound have fixated the ultrasound probe using a headband or a fixation device, to maintain a constant angle of insonation (Clough et al., 2024; Hage et al., 2021; Sorond et al., 2005). Therefore, we used a similar fixation technique (described in the Methods) to avoid changes to the insonation angle during postural changes and minimize this potential source of error in our measurement. We measured MCA velocity (MCAv) as our primary index of CBF, as it is the most commonly measured artery (Aaslid et al., 1982; reviewed in Tymko et al., 2018). Additionally, autoregulation is frequently evaluated using concurrent

comparisons of the velocity of the MCA together with continuous beat-to-beat blood pressure measurements (Aaslid et al., 1982).

1.6 Research Objectives

Primary research objective:

The relationship between hemodynamics and MCAv has been of interest in past literature; however, only non-invasive indices of CO were used. Prior work has shown that both MCAv and CO decrease with orthostatic stress (Edgell et al., 2012), but the extent to which changes in CO contribute to alterations in MCAv remains unclear. Therefore, we directly compared changes in MCAv and invasive CO measurements during the AST in a healthy population. Furthermore, this research provided insight into cardiovascular and cerebrovascular mechanisms during orthostasis and served as a baseline for future comparisons to populations with impaired hemodynamic regulation such as individuals with OI, including POTS and OH.

Secondary research objectives:

Prior studies investigated autonomic responses to changes in posture, reporting increased sympathetic activity and parasympathetic withdrawal (reviewed in Grubb et al., 2008), but the relationship between autonomic changes and MCAv is unclear. The Edgell lab has concurrently recorded heart rate variability (HRV) and MCAv (Robertson et al., 2020); however, we have never tried to link the two directly. Therefore, we assessed the extent to which autonomic mechanisms may contribute to changes in MCAv during the AST. Further, while autoregulation and indices of CBF have been measured while upright (Robertson et al., 2020), the potential role of autoregulation in predicting changes in MCAv during orthostatic stress remains unclear. Consequently, we investigated the association between dynamic cerebral autoregulation in predicting changes in MCAv during the AST.

1.7 Hypotheses

Primary hypothesis:

We hypothesized that during standing, reductions in CO would drive reduced MCAv in a young healthy population of men and women.

Secondary hypotheses:

Due to previous evidence finding that parasympathetic nervous activity causes cerebral vasodilation (Conway et al., 2006), we hypothesized that parasympathetic withdrawal during upright posture would be a predictor of reductions in MCAv. Further, due to previous findings that there are no significant changes of dynamic autoregulation indices while upright (Robertson et al., 2020), we hypothesized that dynamic autoregulation would not predict reductions in MCAv during stand.

Chapter 2: Materials and Methods

2.1 Participants

Healthy younger (between 18-45 years old) and older (>45 years old) adults were recruited from the community. Participants were excluded if they have a history of, or active, cardiovascular, renal, hepatic, pulmonary, systemic, neurological, autonomic, malignant, or musculoskeletal diseases. Male and female participants were ineligible to participate if they use cardioactive medication that is known to influence vascular function and structure, notably beta-adrenoreceptor antagonists, calcium channel blockers, cardiac glycosides, and vasodilators. In order to be considered eligible, women were not taking or using any form of hormone replacement therapy or hormonal contraceptives, including oral contraceptives, hormonal intrauterine device, patches, injections, and implants. The older women recruited were postmenopausal for at least 1 year. Participants were not currently engaging in nor had a recent history (less than 1 year) of ≥ 60 minutes of vigorous resistance or aerobic-based exercise on 5 or more days per week. Participants were also excluded if they were current smokers. All testing was done at the Clinical Cardiovascular Catheterization Research Laboratory at Mount Sinai Hospital, under the supervision of Dr. Susanna Mak (Cardiologist).

2.2 Study Design

This study consisted of two visits. The first visit was comprised of non-invasive hemodynamic and CBF measurements during the AST. The second visit had participants undergo a right heart catheterization procedure with invasive hemodynamic measurements during the AST. Both visits occurred within a 7-day period and Visit 1 was consistently completed prior to Visit 2.

Notably, various factors can influence test results and introduce variability in measurements, including caffeine intake, nicotine, alcohol , recent vigorous exercise (Halliwill et al., 1996), and energy drinks (reviewed in Finucane et al., 2019). Therefore, standardized pre-test conditions and control of these factors are essential to ensure interpretable autonomic responses during the AST. Participants were asked to consume a minimum of 8 cups of liquid (e.g., water, juice) and eat 1800 calories per day, for 3 days prior to testing. For 12 hours before testing, all participants were asked to refrain from drinking alcohol, smoking (e.g., marijuana, cigarettes,

vaping), drinking caffeine (e.g., coffee, tea, energy drinks), and heavy exercise (moderate to vigorous aerobic and resistance training). All participants were asked to fast for 2 hours before arriving for their visit. If both visits were scheduled for one day, participants were asked to consume a light snack (e.g., yogurt, fruit cup) and drink non-caffeinated liquids before their second visit.

2.3 Visit 1 Protocol

During the first visit, informed written consent was obtained and participants completed a screening survey which asked about their self-reported medical history (e.g., medical conditions and prescription medications) and the frequency and intensity of their physical activity per week. A Physical Activity Readiness Questionnaire for Everyone (PAR-Q+) was also completed. Anthropometric data (height and weight) was measured and recorded. Resting HR and seated brachial BP was measured and recorded using a standard automated upper-arm BP cuff (oscillometric method) and ECG (Phillips IntelliVue MP5, Philips Healthcare, Canada). Prior to testing, participants underwent a 12-lead ECG to rule out irregular sinus rhythm and a QRS complex duration of < 110 ms. Participants were instrumented with ECG electrodes, a continuous arterial BP finger cuff (Finometer Pro; Finapres Medical Systems, Arnheim, The Netherlands), a standard brachial BP cuff (Philips Easy M4556B, Philips Healthcare, Canada), a TCD ultrasound probe (Multigon Industries Inc., Yonkers, New York. U.S.A), and a pulse oximeter (Masimo, Irvine, California, U.S.A.) while supine. Participants then performed the AST. First, 5 minutes of baseline measurements were recorded while supine. After baseline, participants moved to a standing position with minimal physical assistance to avoid displacement of the ultrasound probe and the BP finger cuff. Time taken to stand was recorded and the timer was reset once the participant was standing. Participants remained standing unsupported for an additional 10 minutes. Participants were asked to remain still during standing and to refrain from talking throughout the duration of the entire protocol. Participants were asked to sit down if SBP fell below 70 mmHg or at any time they experienced dizziness, nausea, or light-headedness.

2.3.1 Hemodynamic Measurements

Continuous BP measurements were acquired using a non-invasive BP device which used finger-cuff plethysmography (Finometer Pro; Finapres Medical Systems, Arnheim, The Netherlands). The finger cuff was placed on participants' right middle finger which was held at heart level during postural changes using an arm sling to prevent fluid shifts due to gravity. The finger SBP and DBP were externally calibrated to the brachial BP using a standard arm cuff measurement, taken prior to the start of the AST protocol while supine. HR was determined from the R-R interval of a one-lead ECG (BioAmp, ADInstruments, USA).

2.3.2 Indices of Cerebral Blood Flow

Cerebral blood velocity of the MCA was used as the primary index of flow. MCAv was measured with a TCD ultrasound (Multigon Industries Inc., Yonkers, New York). The using a 2-MHz probe positioned at the temporal window and fixated in place using an adjustable headband. MCAv was recorded throughout the duration of the AST.

CPP at the middle cerebral artery was calculated as MAP – (0.7355 mmHg/cmH_2O x distance in cm from the TCD probe to the heart during upright posture) where the clavicle was used as a surrogate placement for the heart), which represents the pressure gradient that drives blood flow through cerebral circulation. The cerebrovascular resistance index (CVRi) was determined to assess resistance to blood flow within the whole cerebral circulation and was calculated by dividing CPP by mean MCAv. Cerebrovascular pulsatility was characterized using the pulsatility index (PI) and resistance index (RI). These indices quantified the pulsatile variation in the blood velocity waveform relative to the mean and maximum flow velocities, respectively (Pahlavian et al., 2021). The PI was assessed as a measure of downstream resistance and was determined as (systolic MCAv– diastolic MCAv)/ mean MCAv. The RI was calculated as (systolic MCAv - diastolic MCAv)/ systolic MCAv, and depicted vascular resistance to blood flow in an artery. Resistance area product (RAP) characterized resistance based on the inverse slope of the linear within-beat arterial BP-MCAv relationship (Robertson et al., 2014) and calculated as (mean CPP – diastolic CPP)/ (mean MCAv– diastolic MCAv). CrCP represented the arterial pressure threshold below which cerebral arteries collapse, resulting in cessation of

blood flow despite the presence of pressure gradient (Burton, 1951). CrCP was calculated as (MAP- RAP)/ mean MCAv.

Cerebral autoregulation was measured by transfer function analysis using Ensemble-R software (Elucimed Ltd., New Zealand). Continuous MCAv and BP recordings were obtained and then were resampled at 4 Hz. Each data set was divided into 4 windows and was passed through a Hanning data window with a 50% overlap. These signals were transformed into frequencies using a fast-Fourier transform to depict specific bands: very low frequency (VLF) (0.02-0.07 Hz), low frequency (LF) (0.07-0.2 Hz), and high frequency (HF) (0.2-0.5 Hz) (Claassen et al., 2016). Spectral analysis also yielded power spectra for mean MCAv and BP. Cross spectral analysis was used to derive the transfer function between mean MCAv and BP to describe how fluctuations in pressure translated to changes in MCAv, through timing (phase) and amplitude (gain). Gain was normalized (nGain) by expressing velocity as a percentage of the mean signal to reduce between-subject variability. A large gain indicated that changes in pressure resulted in greater changes in velocity, and a smaller phase shift indicated that pressure fluctuations were more quickly translated to velocity; both indicating less efficient dynamic autoregulation (Claassen et al., 2016). An additional measure derived from transfer function analysis was coherence, ranging from 0 to 1. Coherence described the reliability of the relationship between gain and phase. Dynamic autoregulation parameters (mean MCAv power, CPP power, gain, nGain, phase, and coherence) were quantified across all the frequency bands (VLF, LF, HF) (Claassen et al., 2016). Ensemble-R software quantified parameters that met a linearity threshold based on a 95% confidence interval.

2.3.3 Heart Rate Variability

Heart rate variability (HRV) analysis was performed as an index of cardiac autonomic function in accordance with established international guidelines (Malik et al., 1996). HRV analyses used data collected during 5 minutes of supine baseline and during the final 5 minutes of the AST, with the HRV module in LabChart software (ADInstruments, Colorado Springs, USA). Time-domain parameters included standard deviation of RR intervals, the root mean square of successive RR interval differences, and the proportion of adjacent RR intervals differing by more than 50 ms (Malik et al., 1996). Frequency-domain measures included total

power, absolute power in the VLF (≤ 0.04 Hz), LF (0.04-0.15 Hz), and HF (0.15-0.4 Hz) bands, LF/HF ratio, and normalized power for LF and HF ranges (Malik et al., 1996). LF reflected both sympathetic and parasympathetic activity, HF reflected parasympathetic activity, and LF/HF reflected the sympathetic control of HR (reviewed in Shaffer & Ginsberg, 2017). Non-linear HRV indices (SD1, SD2, and SD1/SD2) were derived from Poincaré plot geometry to represent total HRV, where SD1 depicted parasympathetic activity and SD2 represented sympathetic input (reviewed in Shaffer & Ginsberg, 2017).

2.3.4 Cardiovagal Baroreceptor Sensitivity

Cardiovagal baroreflex sensitivity (cBRS) was analyzed using the sequence method as an index of baroreflex function. Spontaneous beat-to-beat fluctuations in SBP and RR interval during 5 minutes of supine baseline and last 5 minutes of the AST were analyzed independently. Baroreflex sequences were identified as having at least 3 consecutive heart beats in which both SBP and RR interval decreased or increased (Parati et al., 1988). For each sequence, the increasing ("BRS up") or decreasing ("BRS down") slopes of the relationship between SBP and RR were determined by performing a linear regression analysis. The average "BRS up" and "BRS down" slopes were calculated and combined ("pooled BRS") within supine baseline and during the last 5 minutes of the AST (Ensemble-R, Elucimed Ltd., New Zealand).

2.3.5 Data Acquisition

All hemodynamic and TCD signals were acquired through a PowerLab device at 1000 Hz (ADInstruments, Colorado Springs, CO) and recorded using LabChart software throughout the duration of rest and AST. One-minute averages for hemodynamics and the indices of CBF were taken at minute 4 of supine baseline and at minutes 1, 3, 5, and 10 during standing.

2.4 Visit 2 Protocol

During the second visit, participants were instrumented with ECG electrodes, a brachial BP cuff, a right heart pulmonary catheter, a portable near-infrared spectroscopy (NIRS) device, a portable gas exchange device, and a pulse oximeter while supine (details below). While

participants were being instrumented, they were asked to conduct 10 repetitions of each of the following lower body supine exercises: ankle flexions, ankle extensions, heel slides, ankle rotations (inward and outward) for both legs. Following instrumentation and completion of exercises, participants performed the same AST as described above.

2.4.1 Right Heart Catheterization Procedure

An ultrasound of the upper arm was conducted to assess and confirm accessibility and suitability of the peripheral veins prior to insertion of the catheter. A local anesthetic was administered subcutaneously to the site of venous access. Participants thereafter underwent a right heart catheterization procedure during their second visit. This procedure involved the insertion of a multi-lumen, fluid filled, flotation catheter (Swan-Ganz Oximetry PacePort TD Pulmonary Artery Catheter, Edwards Lifesciences Inc, CA, U.S.A) (Fig. 1) with ultrasound guidance, advancing it into the right heart. Simultaneous pressure waveforms were measured and recorded continuously using the catheter's pressure transducers from the RA, right ventricle (RV), and the PA (Fig. 2). Data was sampled at the 4th minute of supine baseline and at minutes 1, 3, 5 and 10 of standing. Pulmonary artery wedge pressure (PAWP) was measured through intermittent inflation of the balloon tip on the catheter, which was located in a branch of the PA (Fig. 2). The PA balloon was inflated to take PAWP measurements at minute 4 of supine baseline and at minutes 1, 3, 5, and 10 of standing.

Blood oxygen content was obtained from blood samples which were drawn from the distal port located in the main branch of the PA (Fig. 1; Fig. 2). A laser leveling tool was used to establish the phlebostatic axis for transducer placement at the mid-axillary line of the participant in order to measure central venous pressure at the level of the heart. The placement of the arm was adjusted (lowered or raised) ensuring that the position of the transducers remain constantly at the same hydrostatic reference point (at the level of the RA) throughout the postural changes in the protocol to ensure accurate pressure measurements (Fig. 3). Mixed venous blood samples were taken at minute 4 during supine, and during minutes 1, 3, 5, and 10 of standing.

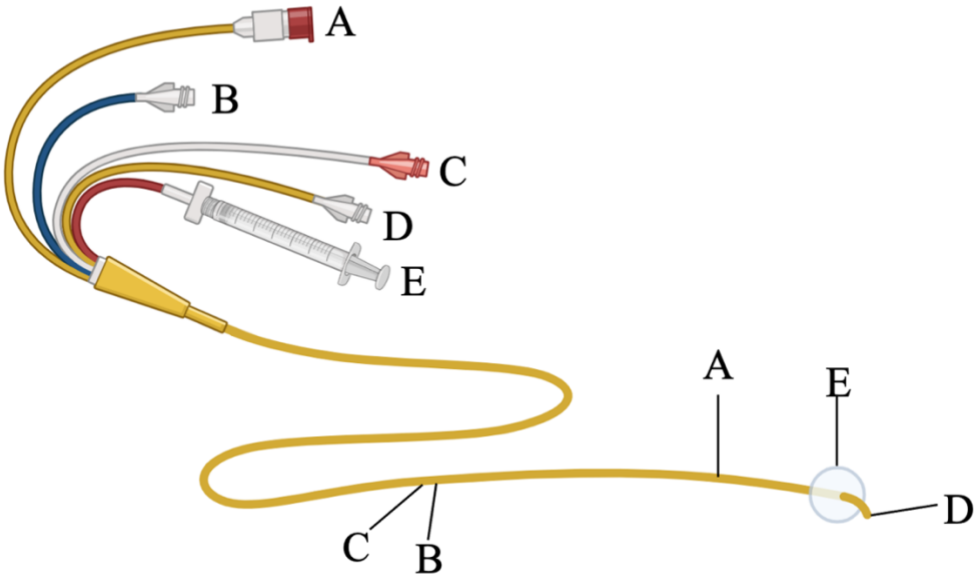

Figure 1. A pulmonary artery catheter with the associated transducers. (A) Thermistor: Measures blood temperature within the pulmonary artery. (B) Proximal Port: Rests in the right atrium of the heart to transduce right atrial pressure and administer fluids (saline) into the right atrium. (C) Right Atrium Infusion Port: Administers IV fluid/medications. (D) Distal Port: Measures pulmonary artery pressure and mixed venous saturation by drawing mixed venous blood samples. (E) Balloon Inflation Port: Inflates balloon located at the catheter's tip. Inflation of the balloon occludes/wedges the distal pulmonary artery allowing for wedge pressure to be obtained. Created with BioRender.com.

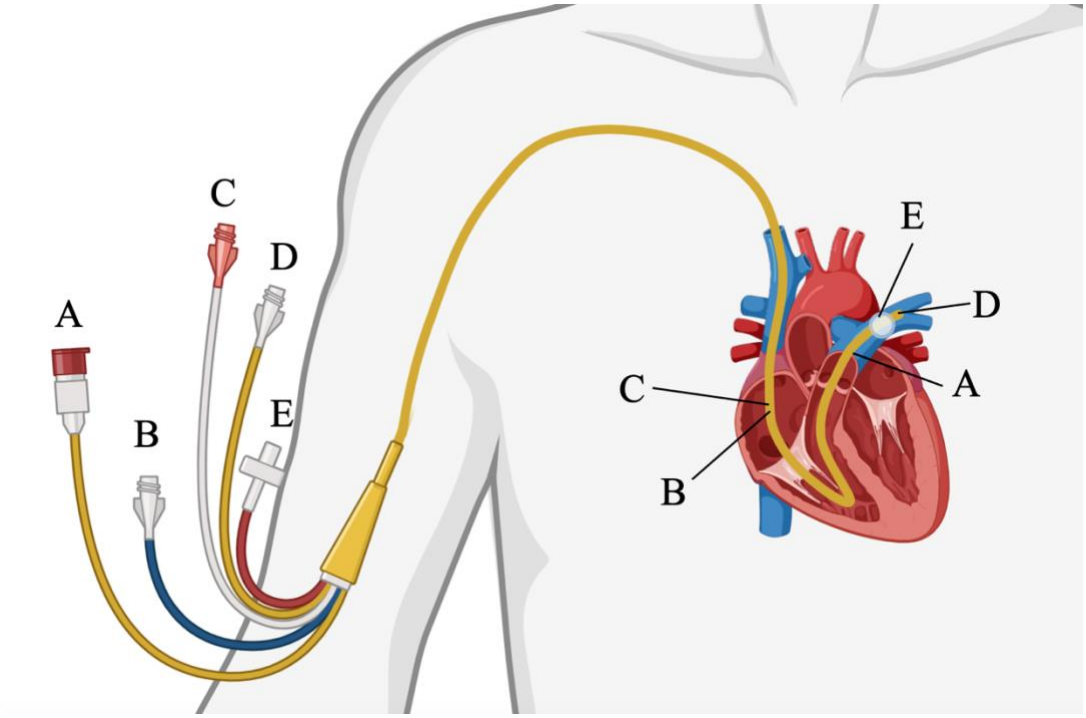

Figure 2. Intracardiac locations of pulmonary catheter transducers. (A) Thermistor: Located approximately 4 cm from the distal tip. (B) Proximal Port: Located approximately 30 cm from the distal tip of the catheter. (C) Right Atrium Infusion Port: Located approximately 31 cm from the distal tip of the catheter. (D) Distal Port: Located at the distal tip of the catheter. (E) Balloon Inflation Port: Located within 2 cm of the distal tip. Created with BioRender.com.

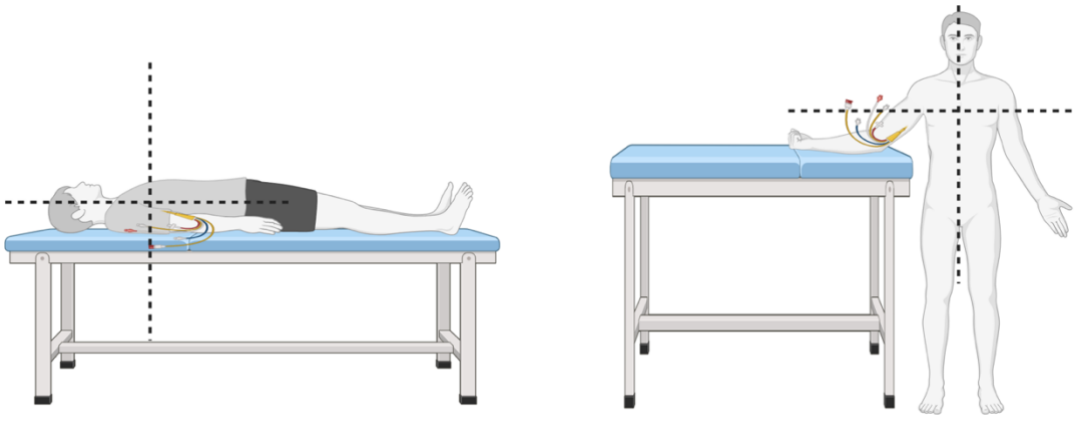

Figure 3. Placement of the arm during Visit 2. During Visit 2, the placement of the arm was adjusted (using the operation room table) throughout the active stand protocol to ensure that the position of the transducers remained constantly at the same hydrostatic reference point (at the level of the right atrium). The hydrostatic indifference point is shown at the intersect of the two black dotted lines. For Visit 1, this was achieved by keeping the Finometer finger blood pressure transducer at the level of the heart using an arm sling. Created with BioRender.com.

2.4.2 Cardiac Output Measurements

2.4.2.1 Thermodilution

During this procedure a known amount of cold saline solution (10 mL at 20°C) was injected into the RA of the heart through the pulmonary catheter (Fig. 1; Fig. 2) and the resulting temperature of the blood which has travelled to the PA was measured by the thermistor at the catheter's tip. The change in temperature of the blood over time was detected and resulted in a temperature-time curve (Fig. 4) where the area under the curve was inversely proportional to CO (Shaffer & Ginsberg, 2017). The blood temperature, saline solution temperature and volume, along with time were used in a Steward-Hamilton equation (Eq. 4) to calculate thermodilution CO (CO_{TD}). CO_{TD} was be measured in triplicate (within $\leq 10\%$ variability) and averaged at baseline (using the 1st and 4th minutes) and during standing (using the 5th and 8th minute of the active stand). From this calculation, stroke volume (SV_{TD}) was calculated as CO_{TD}/HR.

$$CO_{TD} = \frac{V(T_b - T_i)k_1k_2}{\int_{t_1}^{t_2} \Delta T dt} \quad \text{(Eq. 4)}$$

V is volume, T_b is the temperature of blood in the pulmonary artery, T_i is the temperature of the saline injectate, k_1 is the density constant, k_2 is a calibration constant, the integral of $\Delta T dt$ represents the area under the temperature-time curve.

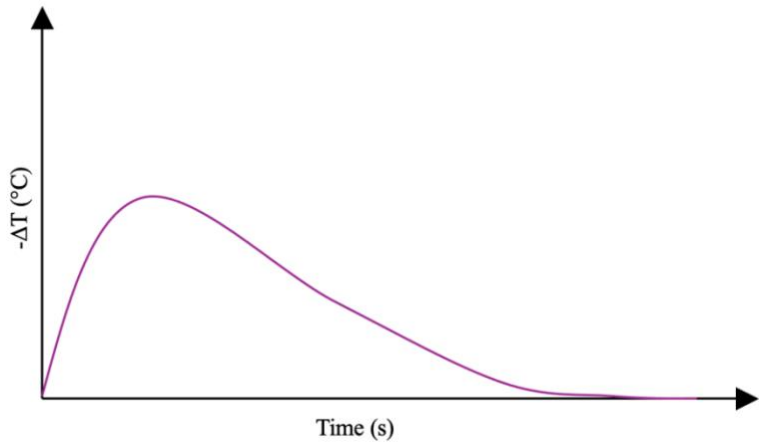

Figure 4. An example of a thermodilution temperature-time curve used to derive CO. Created with BioRender.com.

2.4.2.2 Direct Fick Equation

All participants were fitted with a non-invasive portable gas exchange device (VO_2 Master, VO_2 Master Health Sensors Inc, BC, Canada) which was attached to a standard Hans-Rudolph face mask. This device was tightly secured over the participant's nose and mouth using a head strap to permit continuous breath-by-breath measurements. The size that allowed a flow rate of 5-40 L/min was used. This device measured oxygen consumption (mL O_2/min), breathing frequency (breaths/min), and tidal volume (L), which were used for calculating CO via the direct Fick method (Eq. 5). Direct Fick CO (CO_{DF}) was calculated as the whole body's oxygen consumption divided by the difference between arterial and mixed venous blood oxygen content. The recorded breath-by-breath data was averaged in 30 second bins at minute 4 of the supine condition and at minutes 1, 3, 5, and 10 of standing.

$$CO_{DF} = \frac{\dot{V}O_2}{CaO_2 - CvO_2} \quad \text{(Eq. 5)}$$

$\dot{V}O_2$ represents the oxygen consumed, CaO_2 represents arterial oxygen content, $CvO_2$is mixed venous oxygen content.

Whereas the direct Fick method usually uses an arterial catheter to measures arterial oxygen content (CaO_2), we used a fingertip pulse oximeter. Pulse oximeters have been found to be accurate within 2% (± 1 SD) or 5% (± 2 SD) of arterial blood samples (i.e. analyzed through arterial blood gas test) in the range of 70% to 100% arterial oxygen saturation, with the highest correlation between the two methods in healthy adults (Jensen et al., 1998). Mixed venous blood oxygen was obtained from blood samples from the pulmonary catheter drawn at each of the following timepoints: minute 4 of supine baseline and minutes 1, 3, 5 and 10 of the AST. From this calculation, stroke volume (SV_{DF}) was calculated as CO_{DF}/HR.

2.4.3 Hemodynamic Measurements & Peripheral Muscle Oxygen Saturation

BP measurements were acquired using a standard automated brachial BP arm cuff. HR was determined from the R-R interval of a three-lead ECG (MacLab, GE, Healthcare). BP and

HR measurements were taken at minute 4 of supine baseline and at minutes 1, 3, 5, and 10 during standing.

Peripheral muscle oxygen content was measured throughout the duration of the active stand test using a portable NIRS device (Moxy Monitor, Fortiori Design LLV, MN, U.S.A) fixed in place on the midpoint of the vastus lateralis muscle of either the left or right leg using a bandage. This non-invasive device measured both deoxygenated and total hemoglobin concentrations, which are indicators of blood volume at the local muscle. An increase in total and deoxygenated hemoglobin content in the legs while upright was used as an indicator of venous pooling. Muscle oxygen saturation and total hemoglobin were recorded using one-minute averages at minute 4 of supine baseline and at minutes 1, 3, 5, and 10 during the AST.

2.4.4 Data Acquisition

Hemodynamic parameters including ECG waveforms, HR, pulse oximetry, pulmonary catheter pressures, PA blood temperature measures, and BP were acquired and recorded at 1000 Hz onto a hemodynamic system (MacLab, GE Healthcare, Canada). Continuous oxygen consumption, breathing frequency, tidal volume, and peripheral muscle oxygen saturation measurements were acquired via the VO_2 Master Manager app (Version 0.99.6, VO_2 Master Health Sensors Inc, British Columbia, Canada).

2.5 Data and Statistical Analysis

For each outcome on both testing days, one-way repeated-measures ANOVA were performed to compare baseline hemodynamic, respiratory and cerebral measurements to upright posture in order to assess changes over time. Body mass index (BMI) was calculated as mass (in kilograms) divided by height (in meters) squared. Body surface area (BSA) was calculated using the DuBois and Dubois formula (Eq. 6) (DuBois & DuBois, 1915). A regression analysis was then conducted to assess the presence and strength of any relationship between changing variables with the change in MCAv due to standing. Subsequently, for those variables with $p<0.07$ we also ran a stepwise forward regression to assess the contributions of those factors in predicting changes in MCAv. Significance was defined as $p<0.05$. Normal data were reported as

mean ± SD and non-normal data were presented as median (interquartile range). All statistical analyses were performed using Sigmaplot statistical software (v. 15, San Jose, California, USA).

$$BSA = 0.007184 \times (height\ in\ centimeters)^{0.725} \times (weight\ in\ kilograms)^{0.425}$$

BSA represents body surface area (Eq. 6)

Chapter 3: Results

3.1 Non-Invasive Active Stand Results (Visit 1)

Ten male and six female participants competed the non-invasive AST and are described in Table 1.

Table 1. Participant baseline characteristics on non-invasive testing day.

	All (n=16)
Demographics	
Age (yrs)	47 ± 15
Sex (M:F)	10:6
Height (cm)	173 ± 9
Weight (kg)	73 ± 15
BMI (kg/m^2)	24 ± 4
BSA (m^2)	1.9 ± 0.2
Hemodynamics	
HR (bpm)	61 ± 9
SBP (mmHg)	124 ± 13
DBP (mmHg)	77 ± 7
MAP (mmHg)	93 ± 8

Values are presented as mean ± SD. BMI, body mass index; BSA, body surface area; DBP, diastolic blood pressure; HR, heart rate; MAP, mean arterial blood pressure; M:F, male to female ratio; SBP, systolic blood pressure.

3.1.1 Hemodynamics

HR increased significantly at the first minute of standing and remained elevated across all time points when compared to supine ($p<0.001$; Table 2). There was a significant difference in the change in HR from baseline during standing when comparing minute 1 to minutes 5 ($p<0.05$; Table 2) and 10 ($p<0.05$; Table 2). There were no differences in SBP between supine and any time point during standing ($p=0.101$; Table 2), nor were there any differences in the change from baseline over time ($p=0.709$; Table 2). DBP increased from supine at minute 1 of stand and remained elevated through all following time points ($p<0.001$; Table 2). There were no differences in the change in DBP from baseline over time ($p=0.058$; Table 2). MAP increased significantly from supine to minutes 3, 5 and 10 of standing ($p=0.005$; Table 2); however, there were no differences in the change from baseline when comparing minutes 1, 3, 5, and 10 of standing ($p=0.346$; Table 2). Systolic CPP decreased significantly from supine to minute 1 of standing and remained lower at minutes 3, 5, and 10 of standing ($p<0.001$; Table 2). There were no significant differences in the change in systolic CPP from baseline over time ($p=0.709$; Table 2). Diastolic CPP decreased from supine to minute 1 of standing and remained lower at minutes 3,5, and 10 of standing ($p<0.001$; Table 2). No differences in the change in diastolic CPP from baseline were observed among timepoints during standing ($p=0.0.58$; Table 2). Mean CPP decreased significantly from supine to minute 1 of standing and remained lower at minutes 3,5, and 10 of standing ($p<0.001$; Table 2); there were no differences in the change in mean CPP from baseline over time ($p=0.346$; Table 2).

3.1.2 Cerebrovascular Responses

There was a decrease in systolic MCAv from supine to 1, 3, 5, and 10 minutes of standing ($p<0.001$; Table 2). There were no differences in the change in systolic MCAv from baseline over time ($p=0.510$, Table 2). Diastolic MCAv was not different between supine and the 1st or 3rd minutes of standing but was significantly decreased at the 5th ($p<0.05$; Table 2) and 10th ($p<0.01$; Table 2) minutes of standing. There was no significant differences in the change in diastolic MCAv from baseline over time ($p=0.245$, Table 2). Mean MCAv decreased significantly from supine to minute 1 of standing ($p<0.001$; Table 2) and remained lower across all time points

($p<0.001$, Table 2). There were no significant differences in the change in mean MCAv from baseline over time ($p=0.272$, Table 2).

3.1.3 Cerebral Static Autoregulation

CrCP demonstrated a significant decrease from supine to minutes 1, 3, 5 and 10 ($p<0.01$; Table 2) of standing. There were no significant changes in CVRi, PI, RI, or RAP from supine to any standing timepoint ($p>0.129$; Table 2). There were no significant differences in the changes in CVRi, PI, RI, RAP, and CrCP from baseline among minutes 1, 3,5, and 10 of standing ($p>0.112$; Table 2).

Table 2. Hemodynamic and cerebrovascular responses to the non-invasive active stand test.

	Supine	Stand 1-min	Stand 3-mins	Stand 5-mins	Stand 10-mins	*p*-value
Hemodynamics (n=16)						
HR (bpm)	61 (56-64)	70 (62-79)*	70 (65-84)**	71 (64-83)**	72 (66-82)***	**<0.001**
ΔHR (bpm)	--	10 ± 10	12 ± 10	13 ± 10[a]	13 ± 9[a]	**0.002**
SBP (mmHg)	121 (116-128)	122 (117-132)	125 (119-131)	124 (116-134)	124 (119-133)	0.101
ΔSBP (mmHg)	--	3 ± 8	3 ± 8	4 ± 9	4 ± 9	0.709
DBP (mmHg)	76 (73-83)	86 (81-90)*	86 (81-92)*	86 (81-91)*	88 (81-93)*	**<0.001**
ΔDBP (mmHg)	--	8 ± 5	8 ± 5	9 ± 6	10 ± 6	0.058
MAP (mmHg)	94 (90-101)	100 (96-104)	101 (97-104)*	101 (96-106)*	102 (98-105)*	**0.005**
ΔMAP (mmHg)	--	6 ± 5	6 ± 5	6 ± 6	7 ± 7	0.346
CPP Systolic (mmHg)	121 (166-128)	104 (98-114)***	106 (100-113)***	106 (98-116)***	106 (100-115)**	**<0.001**
ΔCPP Systolic (mmHg)	--	-16 ± 7	-15 ± 8	-15 ± 8	-14 ± 8	0.709
CPP Diastolic (mmHg)	76 (73-83)	68 (63-72)***	68 (62-73)***	68 (62-74)**	70 (62-74)*	**<0.001**
ΔCPP Diastolic (mmHg)	--	-11 ± 5	-10 ± 5	-10 ± 6	-9 ± 6	0.058
Mean CPP (mmHg)	94 (90-101)	82 (78-85)***	83 (78-86)***	83 (77-88)***	83 (80-87)***	**<0.001**
ΔMean CPP (mmHg)	--	-13 ± 5	-12 ± 5	-12 ± 6	-12 ± 6	0.346
Cerebral (n=14)						
MCA Systolic (cm/s)	98 (84-101)	83 (77-92)**	84 (76-97)**	86 (80-94)**	84 (76-96)***	**<0.001**
ΔMCA Systolic (cm/s)	--	-10 (-14- -2)	-7 (-14-1)	-5 (-14- -3)	-5 (-16- -1)	0.510
MCA Diastolic (cm/s)	40 (35-43)	37 (29-43)	37 (31-41)	37 (30-40)*	37 (30-40)**	**0.010**
ΔMCA Diastolic (cm/s)	--	-1.7 ± 3.5	-2.0 ± 3.4	-2.6 ± 3.7	-2.9 ± 4.7	0.245
Mean MCAv (cm/s)	60 (49-66)	52 (47-60)***	54 (45-64)***	53 (47-60)***	53 (45-59)***	**<0.001**
ΔMean MCAv (cm/s)	--	-5.5 ± 5.2	-5.5 ± 5.2	-6.2 ± 4.6	-6.8 ± 5.9	0.272
Static Autoregulation (n=14)						
CVRi (mmHg/cm/s)	1.6 (1.4-1.9)	1.6 (1.3-1.8)	1.6 (1.2-1.9)	1.7 (1.2-1.9)	1.7 (1.3-1.9)	0.378
ΔCVRi (mmHg/cm/s)	--	-0.10 (-0.17- 0.06)	-0.06 (-0.23- 0.05)	-0.09 (-0.18-0.14)	-0.05 (-0.16-0.19)	0.116
PI	0.87 (0.83-1.04)	0.92 (0.73-0.96)	0.86 (0.76-0.98)	0.88 (0.77-1.09)	0.87 (0.76-1.17)	0.129
ΔPI	--	0.01 (-0.08-0.07)	0.01 (-0.04-0.05)	0.02 (-0.07-0.14)	0.01 (-0.06-0.14)	0.258
RI	0.57 (0.54-0.62)	0.56 (0.50-0.61)	0.56 (0.52-0.61)	0.56 (0.52-0.63)	0.56 (0.52-0.65)	0.434
ΔRI	--	-0.01 ± 0.04	-0.01 ± 0.04	-0.00 ± 0.05	0.00 ± 0.01	0.112
RAP (mmHg/cm/s)	0.88 ± 0.24	0.92 ± 0.27	0.91 ± 0.25	0.90 ±0.25	0.90 ± 0.22	0.786

ΔRAP (mmHg/cm/s)	--	0.05 (-0.05-0.18)	0.00 (-0.03-0.08)	-0.01 (-0.05-0.07)	0.01 (-0.40-0.04)	0.896
CrCP (mmHg)	44 ± 14	34 ± 6***	35 ± 16***	37 ± 14***	38 ± 14**	**<0.001**
ΔCrCP (mmHg)	--	-11 (-14- -5)	-10 (-13- -4)	-10 (-12- -2)	-8 (-14-2)	0.112

Normal data are reported as mean ± SD and non-normal data as median (interquartile range). p-values are from one-way repeated measures ANOVA. Tukey post-hoc tests vs. supine baseline ($p<0.05$*, $p<0.01$**, $p<0.001$***). Δ values present Stand – Supine. CPP, cerebral perfusion pressure; CrCP, critical closing pressure; CVRi, cerebrovascular resistance index; DBP, diastolic blood pressure; HR, heart rate; MAP, mean arterial blood pressure; MCA, middle cerebral artery; MCAv, mean middle cerebral artery velocity; PI, pulsatility index; RAP, resistance area product; RI, resistance index; SBP, systolic blood pressure. *a* indicates significant difference from Stand 1-min.

3.1.4 Cerebral Dynamic Autoregulation

The data presented in Table 3 reflect measures at supine and for the last 5 minutes of standing. There were no significant changes from supine to stand in any of the HF dynamic autoregulation parameters ($p>0.620$; Table 3). Across the LF band, there was a significant increase in BP power from supine to stand ($p=0.006$), but there were no significant differences in mean MCAv power, gain, nGain, phase, or coherence ($p>0.052$; Table 3). VLF gain and nGain decreased significantly from supine to stand ($p<0.014$; Table 3). VLF phase significantly decreased from supine to stand ($p=0.006$; Table 3) and VLF coherence decreased significantly between the supine position and standing ($p=0.041$; Table 3).

Table 3. Spectral and transfer function analysis of blood pressure and MCAv during the non-invasive active stand test.

Cerebral Dynamic Autoregulation		Supine	n	Stand	n	*p*-value
HF (0.2-0.4 Hz)	BP Power ($mmHg^2$)	1.5 ± 1.3	15	1.5 ± 0.9	14	0.766
	ΔBP Power ($mmHg^2$)	--	--	-0.1 ± 1.1	14	--
	Mean MCAv Power (cm^2/s^2)	2.3 ± 3.2	15	2.0 ± 1.6	14	0.726
	ΔMean MCAv Power (cm^2/s^2)	--	--	-0.3 ± 3	14	--
	Gain (cm/s/mmHg)	1.0 ± 0.8	12	1.1 ± 0.7	12	0.665
	ΔGain (cm/s/mmHg)	--	--	-0.1 ± 0.7	10	--
	nGain (%/mmHg)	1.6 ± 1.2	12	2.3 ± 1.7	12	0.817
	ΔnGain (%/mmHg)	--	--	0.1 ± 1.0	10	--
	Phase (radians)	0.1 ± 0.3	12	0.3 ± 0.7	12	0.620
	ΔPhase (radians)	--	--	-0.1 ± 0.4	10	--
	Coherence (au)	0.4 ± 0.2	15	0.4 ± 0.2	14	0.646
	ΔCoherence (au)	--	--	0.0 ± 0.2	14	--
LF (0.07-0.2 Hz)	BP Power ($mmHg^2$)	3.2 ± 1.8	15	7.2 ± 5.3	14	**0.006**
	ΔBP Power ($mmHg^2$)	--	--	4.0 ± 4.6	14	--
	Mean MCAv Power (cm^2/s^2)	5.6 ± 4.7	15	8.2 ± 7.3	14	0.116
	ΔMean MCAv Power (cm^2/s^2)	--	--	3.0 ± 6.7	14	--
	Gain (cm/s/mmHg)	1.0 ± 0.4	15	1.3 ± 1.4	14	0.817
	ΔGain (cm/s/mmHg)	--	--	0 ± 0.3	12	--
	nGain (%/mmHg)	1.6 ± 0.6	13	2.8 ± 4.3	14	0.304
	ΔnGain (%/mmHg)	--	--	0.1 ± 0.4	12	--
	Phase (radians)	0.6 ± 0.6	13	0.6 ± 0.2	14	0.254
	ΔPhase (radians)	--	--	-0.1 ± 0.3	12	--
	Coherence (au)	0.5 ± 0.2	15	0.6 ± 0.1	14	0.052

	ΔCoherence (au)	--	--	0.1 ± 0.2	14	--
VLF (0.02-0.07 Hz)	BP Power ($mmHg^2$)	7.0 ± 5.4	15	9.1 ± 7.3	14	0.279
	ΔBP Power ($mmHg^2$)	--	--	1.9 ± 6.2	14	--
	Mean MCAv Power (cm^2/s^2)	10.2 ± 8.6	15	7.9 ± 5.4	14	0.719
	ΔMean MCAv Power (cm^2/s^2)	--	--	-0.7 ± 6.7	14	--
	Gain (cm/s/mmHg)	1.2 ± 0.4	10	0.8 ± 0.2	13	**0.002**
	ΔGain (cm/s/mmHg)	--	--	-0.4 ± 0.3	11	--
	nGain (%/mmHg)	2.1 ± 0.8	10	1.5 ± 0.3	13	**0.014**
	ΔnGain (%/mmHg)	--	--	-0.7 ± 0.7	10	--
	Phase (radians)	1.3 ± 0.4	10	1.0 ± 0.4	13	**0.006**
	ΔPhase (radians)	--	--	-0.4 ± 0.4	10	--
	Coherence (au)	0.4 ± 0.1	14	0.5 ± 0.1	14	**0.041**
	ΔCoherence (au)	--	--	0.1 ± 0.2	14	--

Values are presented as mean ± SD. au, arbitrary units; BP, blood pressure; HF, high frequency; LF, low frequency; MCAv, mean middle cerebral artery velocity; nGain, normalized gain; VLF, very low frequency.

3.1.5 Cardiac Autonomic Function Measures

HRV analysis was used to assess cardiac autonomic function for 5 minutes of the supine position and last 5 minutes of standing. Within the time domain, RR mean decreased significantly from supine to standing ($p<0.001$), SDRR decreased with standing ($p=0.003$), and no significant differences were observed in NN50, pNN50, and RMSSD with standing ($p>0.052$; Table 4). Within the frequency domain, the normalized HF band decreased from supine to standing ($p=0.018$), yet there were no differences between supine to standing in other frequencies (LF and VLF) nor the index of sympathetic activity (LF/HF; $p>0.059$; Table 4). For non-linear measures of HRV, only long-term variability SD2 was observed to decrease significantly ($p=0.022$; Table 4) when standing.

cBRS was analyzed during supine and for the last 5 minutes of stand. There was a significant decrease of "BRS up" from supine to stand ($p=0.009$) with a significant decrease of "BRS down" from supine to standing ($p=0.021$; Table 5). As such, there was a significant decrease in "pooled BRS" from supine to standing ($p=0.012$; Table 5).

Table 4. HRV during the non-invasive active stand test (n=16).

	Supine	**Stand**	***p*-value**
Time Domain			
NN50	54 ± 62	26 ± 35	0.072
ΔNN50	--	-28 ± 57	--
pNN50 (%)	20 ± 24	8 ± 11	0.052
ΔpNN50 (%)	--	-11.5 ± 22	--
RMSSD (ms)	54 ± 54	30 ± 25	0.121
ΔRMSSD (ms)	--	-24 ± 57	--
RR Mean (s)	1.0 ± 0.2	0.8 ± 0.2	**<0.001**
ΔRR Mean (s)	--	-0.2 ± 0.1	--
SDRR (ms)	66 ± 42	39 ± 17	**0.003**
ΔSDRR (ms)	--	-28 ± 31	--
Frequency Domain			
VLF power (ms^2)	486 ± 726	239 ± 276	0.171
ΔVLF power (ms^2)	--	-247 ± 687	--
LF power (ms^2)	763 ± 1222	415 ± 362	0.207
ΔLF power (ms^2)	--	-348 ± 1057	--
LF (nu)	56 ± 20	70 ± 17	0.059
ΔLF (nu)	--	13 ± 26	--
HF power (ms^2)	732 ± 1694	245 ± 485	0.286
ΔHF power (ms^2)	--	-486 ± 1759	--
HF (nu)	41 ± 19	26 ± 13	**0.018**
ΔHF (nu)	--	15 ± 22	--
LF/HF	2.1 ± 2.1	3.6 ± 2.1	0.075
ΔLF/HF	--	1.4 ± 3	--
Poincaré plot			
SD1 (ms)	38 ± 38	22 ± 18	0.121
ΔSD1 (ms)	--	-17 ± 41	--
SD2 (ms)	84 ± 49	57 ± 25	**0.022**
ΔSD2 (ms)	--	-27 ± 43	--
SD2/SD1	2.6 ± 1.0	3.5 ± 1.8	0.164
ΔSD2/SD1	--	0.8 ± 2.2	--

Data are presented as mean ± SD. HF, high frequency; LF, low frequency; LF/HF, ratio of low to high frequency components of heart rate variability; NN50, absolute number of NN intervals greater than 50 ms; nu, normalized units; pNN50, the percentage of NN intervals greater than 50 ms; RMSSD, square root of the mean of the sum of squared differences between RR intervals;

SD1, standard deviation of the short-term NN interval variability; SD2, standard deviation of the long-term NN interval variability; SDRR, standard deviations of all RR intervals; VLF, very low frequency.

Table 5. Cardiovagal baroreceptor sensitivity (cBRS) during the non-invasive active stand test (n=16).

	Supine	**Stand**	***p*-value**
Time Domain			
BRS up (ms/mmHg)	30 ± 25	12 ± 7	**0.009**
ΔBRS up (ms/mmHg)	--	-19 ± 25	--
BRS down (ms/mmHg)	28 ± 27	11 ± 6	**0.021**
ΔBRS down (ms/mmHg)	--	-16 ± 25	--
BRS pooled (ms/mmHg)	29 ± 25	12 ± 6	**0.012**
ΔBRS pooled (ms/mmHg)	--	-17 ± 24	--

Data are presented as mean ± SD. BRS, cardiovascular baroreceptor sensitivity.

3.1.6 Comparisons of the Change of Mean Cerebral Blood Velocity to the Changes of Hemodynamic, Cerebrovascular, and Autonomic Variables with Standing

The Δ mean MCAv due to 5 minutes of standing was not associated with ΔHR, ΔSBP, ΔDBP, or ΔMAP ($p>0.261$; Table 6). As expected, Δ mean MCAv demonstrated a strong positive correlation with Δ systolic ($r=0.908$, $p<0.001$; Table 6; Fig. 5) and Δ diastolic ($r=0.768$, $p=0.001$; Table 6; Fig. 6) MCAv. Δ mean MCAv was also significantly inversely correlated with the ΔCVRi ($r=-0.816$, $p<0.001$; Table 6; Fig. 7). There were no relationships between Δ mean MCAv and changes in other cerebrovascular hemodynamic variables and resistance indices (ΔSystolic CPP, ΔDiastolic CPP, mean ΔCPP, ΔPI, ΔRI, ΔRAP, ΔCrCP; $p>0.210$; Table 6). There were no significant relationships between Δ mean MCAv and the changes of cerebral dynamic autoregulation (ΔHF, ΔLF or ΔVLF power, gain, nGain, phase, coherence; $p>0.063$; Table 6); however, there were two notable trends where Δ mean MCAv tended to positively relate to the ΔHF phase ($r=0.607$, $p=0.063$; Table 6) and tended to negatively relate to ΔVLF nGain ($r=-0.583$, $p=0.077$; Table 6). When both variables (ΔHF phase and ΔVLF nGain) were subsequently forced into a stepwise forward regression model against the Δ mean MCAv, ΔHF phase was a significant predictor of Δ mean MCAv ($p=0.010$; Fig. 8), whereas ΔVLF nGain was not significant ($p=0.074$). Additionally, there were no significant relationships between changes of autonomic activity during standing (ΔHRV or ΔBRS) and Δ mean MCAv ($p>0.209$; Table 6).

Table 6. Linear regression analysis of mean MCAv and hemodynamic, cerebrovascular, and autonomic measures during the non-invasive active stand test.

Independent Variable	**Dependent Variables**		**r**	**R^2**	***p*-value**
	Hemodynamics				
ΔMean MCA (cm/s)	ΔHR (bpm)		0.166	0.028	0.571
	ΔSBP (mmHg)		0.322	0.104	0.261
	ΔDBP (mmHg)		-0.103	0.011	0.725
	ΔMAP (mmHg)		0.134	0.018	0.648
	Cerebrovascular Hemodynamics				
	ΔMCA Systolic (cm/s)		0.908	0.825	**<0.001**
	ΔMCA Diastolic (cm/s)		0.768	0.590	**0.001**
	ΔCPP Systolic (mmHg)		0.067	0.004	0.821
	ΔCPP Diastolic (mmHg)		-0.113	0.013	0.701
	ΔCPP (mmHg)		0.129	0.017	0.660
	ΔCVRi (mmHg/cm/s)		-0.816	0.666	**<0.001**
	ΔPI		-0.323	0.105	0.259
	ΔRI		-0.247	0.061	0.395
	ΔRAP (mmHg/cm/s)		-0.004	0.000	0.990
	ΔCrCP (mmHg)		-0.357	0.127	0.210
	Cerebral Autoregulation				
	ΔHF (0.2-0.4 Hz)	ΔBP Power ($mmHg^2$)	0.380	0.144	0.180
		ΔMean MCAv (cm^2/s^2)	-0.407	0.166	0.149
		ΔGain (cm/s/mmHg)	-0.166	0.027	0.647
		ΔnGain (%/mmHg)	-0.175	0.031	0.628

		ΔPhase (radians)	0.607	0.369	0.063
		ΔCoherence (au)	0.362	0.131	0.203
	ΔLF (0.07-0.2 Hz)	ΔBP Power ($mmHg^2$)	0.231	0.053	0.427
		ΔMean MCAv (cm^2/s^2)	0.023	0.001	0.937
		ΔGain (cm/s/mmHg)	0.081	0.007	0.802
		ΔnGain (%/mmHg)	0.009	0.000	0.979
		ΔPhase (radians)	-0.168	0.028	0.603
		ΔCoherence (au)	0.124	0.015	0.673
	ΔVLF (0.02-0.07 Hz)				
		ΔBP Power ($mmHg^2$)	-0.332	0.110	0.246
		ΔMean MCAv (cm^2/s^2)	-0.442	0.196	0.113
		ΔGain (cm/s/mmHg)	-0.495	0.245	0.146
		ΔnGain (%/mmHg)	-0.583	0.340	0.077
		ΔPhase (radians)	-0.504	0.254	0.137
		ΔCoherence (au)	-0.075	0.006	0.799
	Baroreflex Sensitivity				
	ΔBRS up (ms/mmHg)		-0.358	0.128	0.209
	ΔBRS down (ms/mmHg)		-0.265	0.070	0.360
	ΔBRS pooled (ms/mmHg)		-0.293	0.086	0.310
	HRV				
	Time Domain				
		ΔNN50	-0.043	0.002	0.884
		ΔpNN50 (%)	-0.039	0.002	0.894
		ΔRMSSD (ms)	0.116	0.013	0.694
		ΔRR Mean (s)	-0.057	0.003	0.847
		ΔSDRR (ms)	0.033	0.001	0.912
	Frequency Domain				

		ΔVLF power (ms^2)	-0.142	0.020	0.628
		ΔLF power (ms^2)	0.037	0.001	0.900
		ΔHF power (ms^2)	0.053	0.003	0.857
		ΔnLF (nu)	-0.076	0.006	0.796
		ΔnHF (nu)	0.049	0.002	0.869
		ΔLF/HF (ratio)	0.299	0.089	0.299
		ΔVLF (%)	-0.204	0.042	0.484
		ΔLF (%)	0.056	0.003	0.850
		ΔHF (%)	0.149	0.022	0.612
	Poincaré plot				
		ΔSD1 (ms)	0.116	0.013	0.694
		ΔSD2 (ms)	0.330	0.109	0.250
		ΔSD2/SD1	0.062	0.004	0.834

au, arbitrary units; BP, blood pressure; BRS, cardiovascular baroreceptor sensitivity; CPP, cerebral perfusion pressure; CrCP, critical closing pressure; CVRi, cerebrovascular resistance index; DBP, diastolic blood pressure; HR, heart rate; MAP, mean arterial blood pressure; MCA, middle cerebral artery; MCAv, mean middle cerebral artery velocity; nGain, normalized gain; (n)HF, (normalized) high frequency; (n)LF, (normalized) low frequency; nu, normalized units; (p)NN50, the (percentage of) NN intervals greater than 50 ms; PI, pulsatility index; RAP, resistance area product; RI, resistance index; RMSSD, square root of the mean of the sum of squared differences between RR intervals; SBP, systolic blood pressure; SD1, standard deviation of the short-term NN interval variability; SD2, standard deviation of the long-term NN interval variability; SDRR, standard deviations of all RR intervals; VLF, very low frequency.

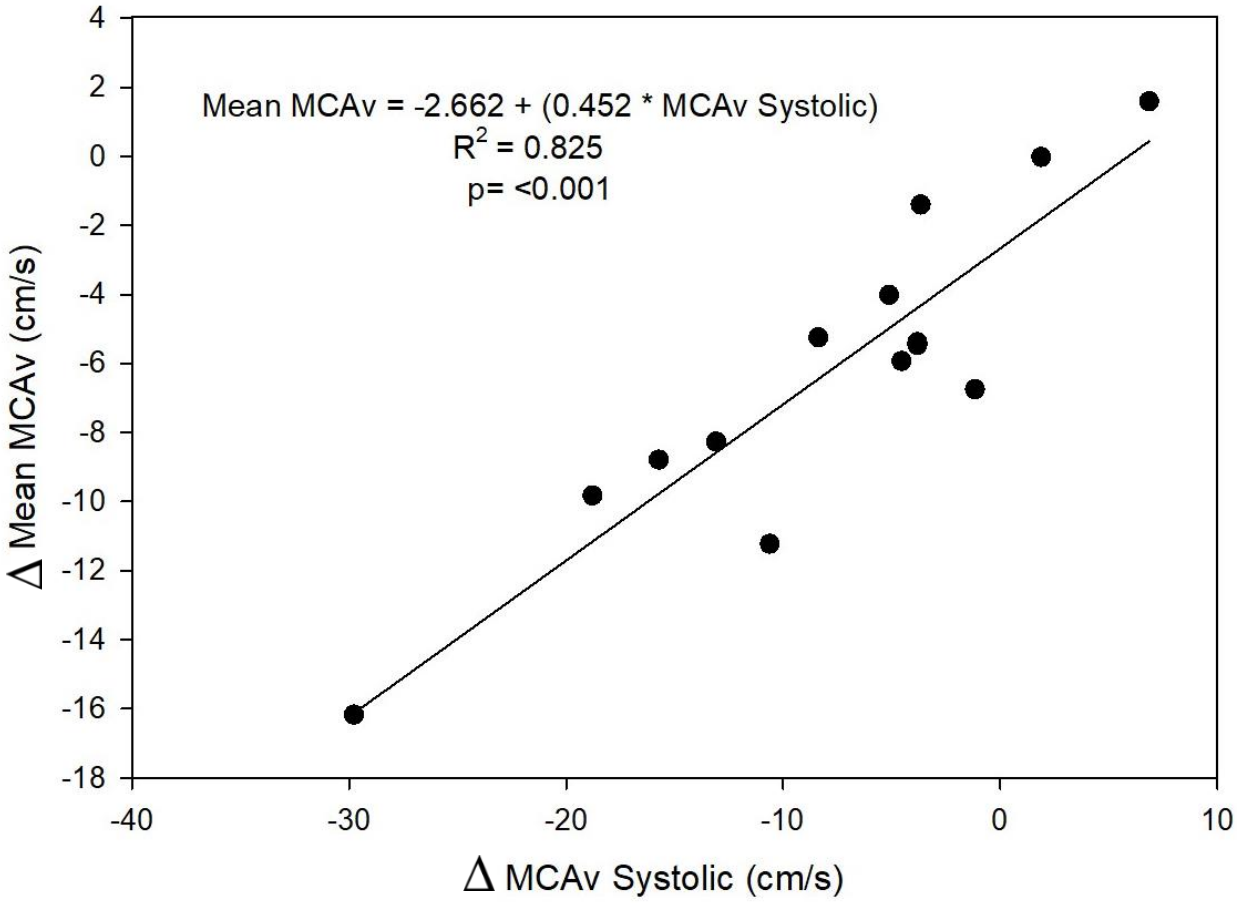

Figure 5. Association between changes in systolic middle cerebral artery velocity (MCAv) and mean MCAv due to standing.

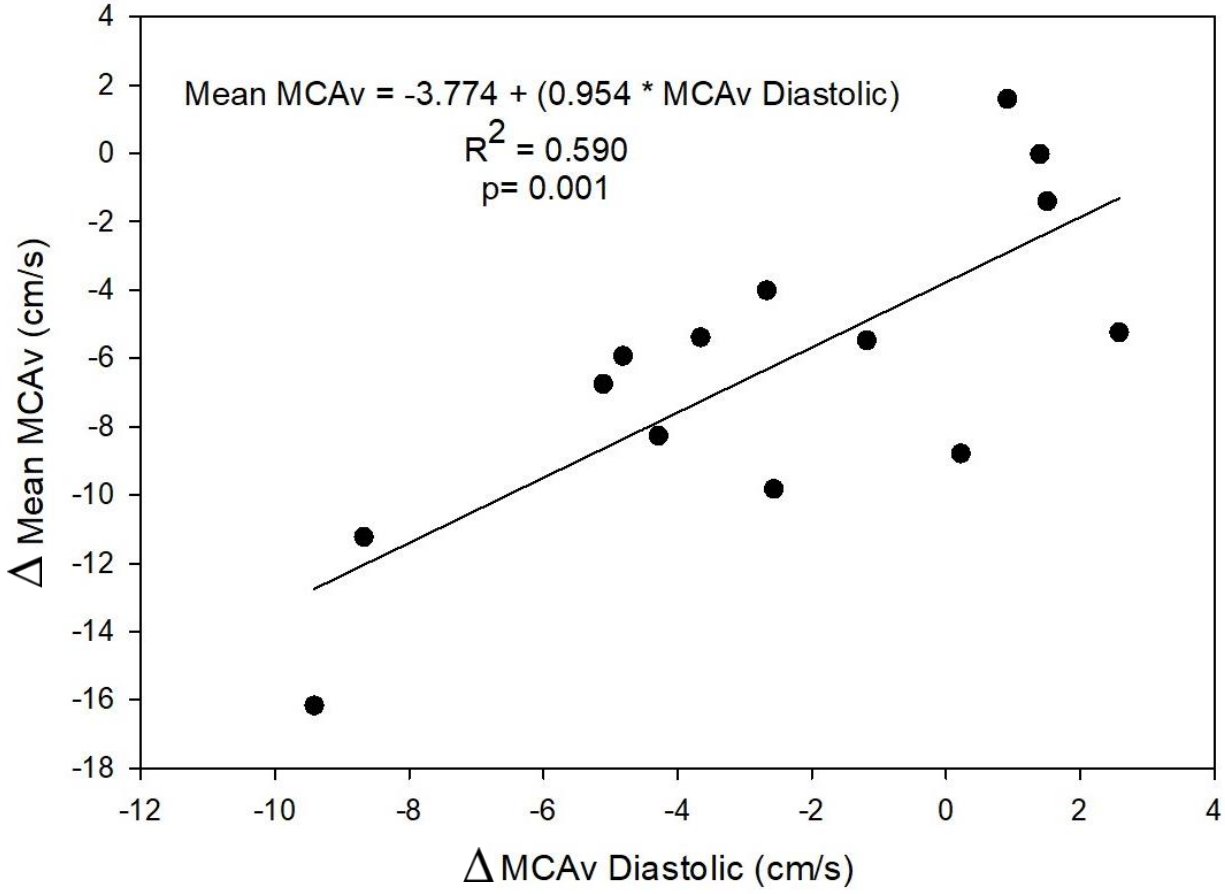

Figure 6. Association between changes in diastolic middle cerebral artery velocity (MCAv) and mean MCAv due to standing.

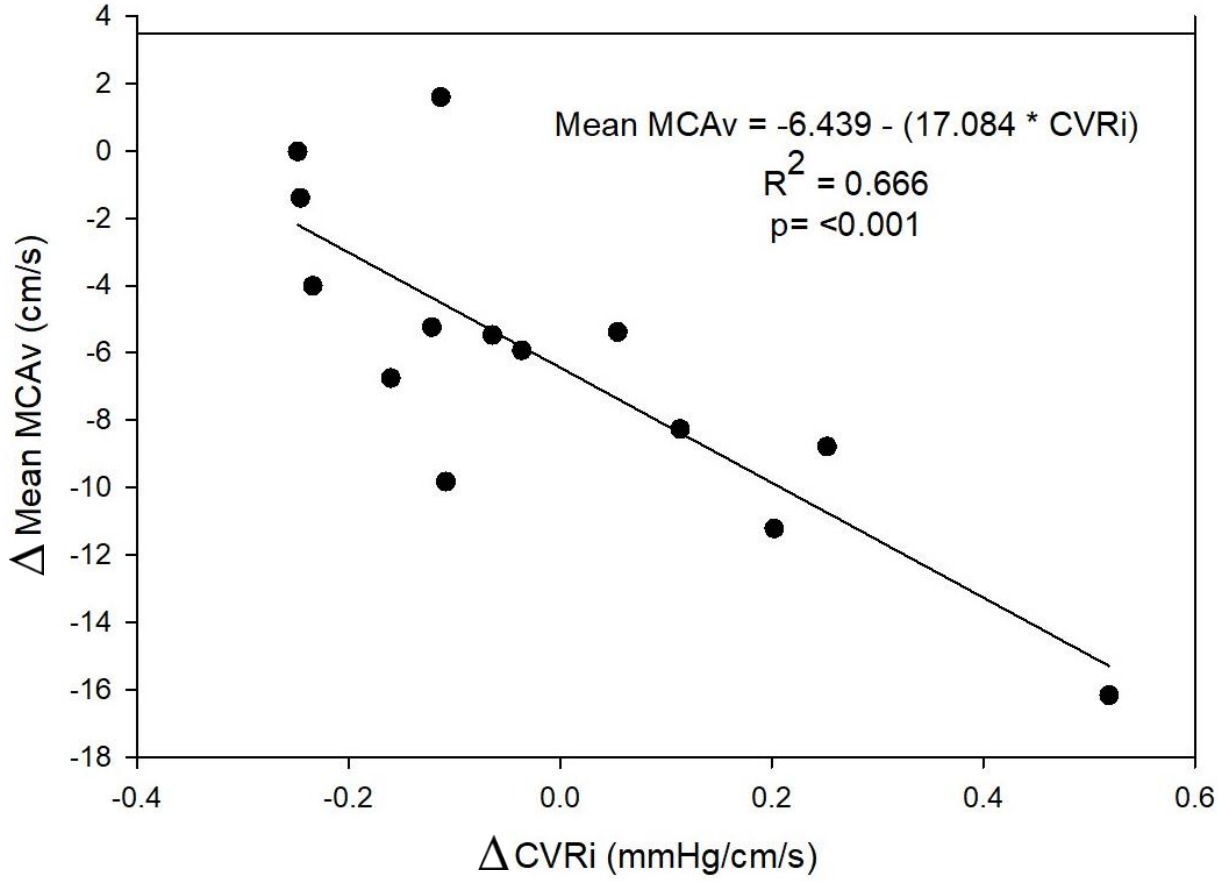

Figure 7. Association between changes in cerebrovascular resistance index (CVRi) and mean middle cerebral artery velocity (MCAv) due to standing.

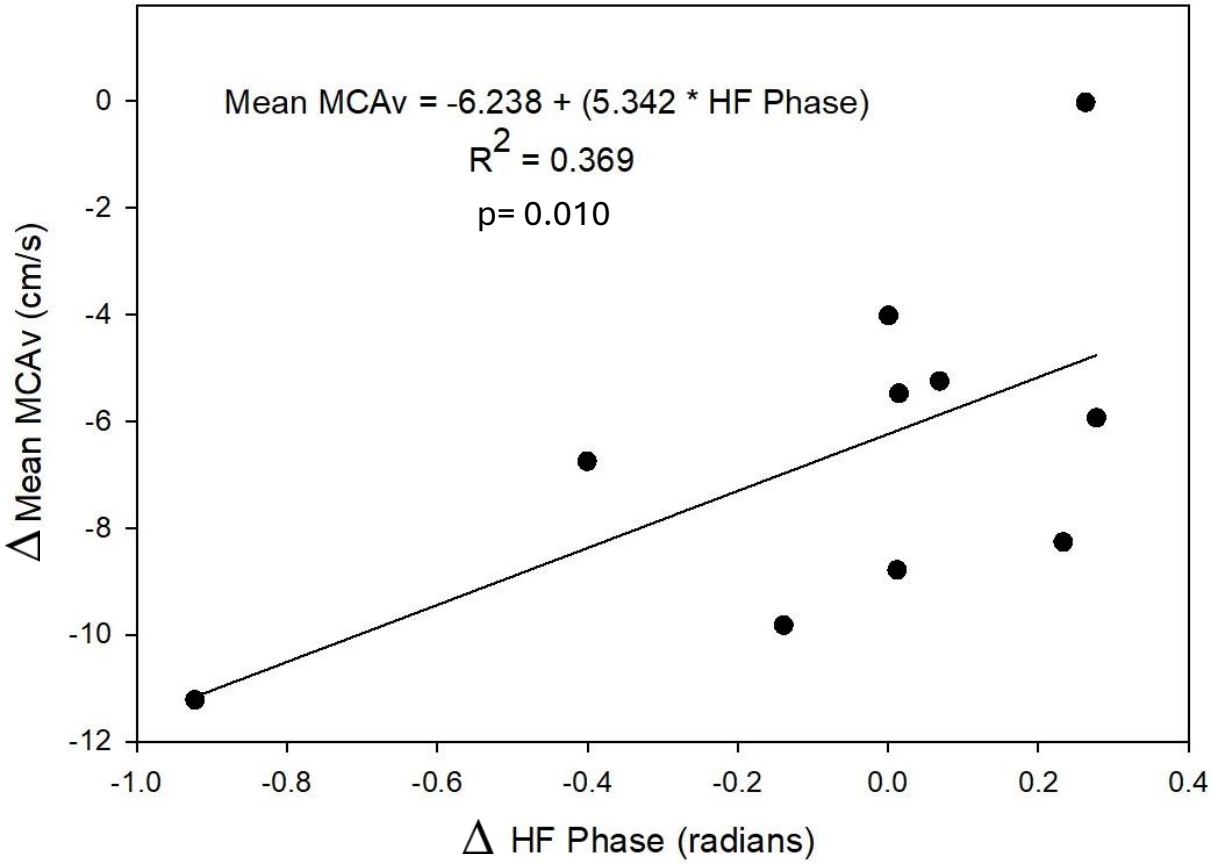

Figure 8. Association between changes in high frequency (HF) phase and mean middle cerebral artery velocity (MCAv) due to standing.

3.2 Invasive Active Stand Results (Visit 2)

Nine male and five female participants competed the invasive AST and are described in Table 7.

Table 7. Participant baseline characteristics on the invasive testing day.

	All (n=14)
Demographics	
Age (yrs)	47 ± 15
Sex (M:F)	9:5
Height (cm)	173 ± 9
Weight (kg)	74 ± 16
BMI (kg/m^2)	25 ± 4
BSA (m^2)	1.9 ± 0.3
Hemodynamics	
HR (bpm)	60 ± 8
SBP (mmHg)	123 ± 13
DBP (mmHg)	78 ± 7
MAP (mmHg)	93 ± 8
Ventilation	
V_E (L/min)	8.8 ± 1.8
V_Ei (L/min/m^2)	4.7 ± 0.7
Tv (L)	0.6 ± 0.1
Rf (breath/min)	17 ± 3
VO_2 (mL/min)	262 ± 51
VO_2 (mL/kg/min)	3.6 ± 0.7
Peripheral Oxygenation	
THb (au)	12.1 ± 0.7
O_2Hb (au)	8.5 ± 1.7
HHb (au)	3.6 ± 2.1

SmO_2 (%)	71 ± 16

Values are presented as mean ± SD. au, arbitrary units; BMI, body mass index; BSA, body surface area; DBP, diastolic blood pressure; HHb, relative deoxyhemoglobin; HR, heart rate; MAP, mean arterial blood pressure; O_2Hb, relative oxyhemoglobin; Rf, respiratory frequency; SBP, systolic blood pressure; SmO_2, vastus lateralis muscle oxygenation; THb, relative total hemoglobin; Tv, tidal volume; V_E, minute ventilation; V_Ei, minute ventilation indexed to BSA; VO_2, oxygen uptake.

3.2.1 Hemodynamics

There was a significant increase in HR from supine to the first minute of standing, with HR remaining elevated throughout the duration of the stand test ($p<0.001$; Table 8). There were no differences observed in the change in HR from baseline across time ($p=0.374$; Table 8). SBP decreased significantly at 10 minutes of standing from supine ($p=0.010$; Table 8). The change in SBP from baseline at minute 10 of standing was significantly greater than the changes at minutes 1 and 3 of standing ($p<0.05$; Table 8). There were no significant differences in DBP and MAP between supine and any time point during standing ($p>0.180$; Table 8), nor were there any differences in the changes from baseline over time ($p>0.074$; Table 8) in both variables.

3.2.2 Cardiac Output Measurements

CO measured by thermodilution significantly decreased from supine to 5 minutes of standing ($p<0.001$; Table 8). Direct Fick CO demonstrated a significant initial decrease from supine after 1 minute of standing and remained significantly lower than supine at all timepoints ($p<0.001$; Table 8). There were no differences in the change in direct Fick derived CO from baseline across standing ($p=0.557$; Table 8). SV derived from thermodilution decreased significantly from supine to 5 minutes of standing $p<0.001$; Table 8). Direct Fick derived SV decreased significantly from supine to 1 minute of standing and remained lower across all the time points when compared to the supine value ($p<0.001$; Table 8). There were no significant differences in the change in direct Fick derived SV from baseline over time ($p=0.520$; Table 8).

3.2.3 Pulmonary Blood Pressures

RaP decreased from supine after 1 minute of standing and remained significantly lower than the supine measurement at all timepoints ($p<0.001$; Table 8). There were no differences in the change in RaP from baseline over all standing timepoints ($p=0.750$: Table 8). There was a significant decrease in RVSP from supine after 3 minutes of standing ($p<0.001$; Table 8) which remained lower for subsequent timepoints such that the change in RVSP from baseline was lower at 5 and 10 minutes compared to the first minute of standing ($p<0.001$; Table 8). RVDP decreased from supine after 3 minutes of standing and remained lower for minutes 5 and 10 of standing ($p<0.001$; Table 8). The change in RVDP from baseline at minutes 5 and 10 of standing

were significantly greater than the changes at minutes 1 and 3 of standing (p=0.009; Table 8). RVEDP decreased significantly from supine to 1 minute of standing and remined lower for all subsequent timepoints (p<0.001; Table 8). No differences were observed in the change in RVEDP from baseline over time (p=0.352; Table 8). During standing, both PASP and PADP decreased significantly after 1 minute of standing and remained lower through all following time points (p<0.011: Table 8). Additionally, there was a significantly greater change in PASP from baseline at 10 minutes of standing compared to 1 minute of standing (p=0.012; Table 8) but there were no differences in the change in PADP from baseline over time (p=0.380; Table 8). mPAP decreased from supine to 1 minute of standing which remained statistically lower throughout all time points (p=0.011; Table 8). There was a main effect of time in the change in mPAP from baseline (p=0.013; Table 8), but pairwise comparisons did not show any significant differences (p>0.059).. PAWP decreased significantly from supine to 1 minute of standing and remained lower for the duration of the 10-minute stand test (p<0.001; Table 8). There was a significantly greater change in PAWP from baseline at 10 minutes of standing compared to 1 minute of standing (p=0.007; Table 8).

3.2.4 Blood Oximetry

There was no significant change in SaO_2 when comparing supine to standing (p=0.996; Table). When examining the change in SaO_2 from baseline, there was a significant main effect of time (p=0.021; Table 8); but pairwise comparisons did not show any significant differences (p>0.339). There was no significant change in CaO_2 from supine to minutes 1, 3, 5, and 10 of standing (p=1.000; Table 8). There was a significant main effect of time on the change in CaO_2 from baseline to minutes 1, 3 5, and 10 of standing (p=0.014; Table 8), but pairwise comparisons did not reveal any significant differences (p>0.262). SvO_2 decreased from supine to 1 minute of standing and remained lower across the subsequent time points (p<0.001; Table 8). There were no differences in the change in SvO_2 from baseline across time (p=0.733; Table 8). CvO_2 decreased from supine at 1 minute of standing and remained lower across subsequent timepoints (p<0.001; Table 8). There were no differences in the change in CvO_2 from baseline across time (p=0.733; Table 8).

3.2.5 Peripheral Muscle Oxygenation

SmO_2 significantly decreased at 1 minute of standing and remained lower throughout the rest of the stand ($p<0.001$; Table 8). There was a significantly greater change in SmO_2 from baseline at 5 minutes of standing compared to 1 minute of standing ($p=0.032$; Table 8). THb increased significantly after 5 minutes of standing ($p<0.001$; Table 8) and was significantly higher at minute 10 of standing when compared to minute 1 of standing ($p<0.05$; Table 8). Change in THb from baseline at minutes 5 and 10 of standing were significantly greater than the changes at minutes 1 and 3 ($p<0.001$; Table 8). O_2Hb decreased from supine to 3 minutes of standing and remained lower for the rest of the time points ($p<0.001$; Table 8). The change in O_2Hb from baseline at minute 5 of standing was significantly greater than the change at minute 1 of standing ($p=0.032$; Table 8). HHb increased from supine to 1 minute of standing and remained elevated for the duration of standing ($p<0.001$; Table 8). Additionally, HHb was elevated at minutes 5 and 10 of standing compared to minute 1 of standing ($p<0.05$; Table 8). There was a significantly greater change in HHb from baseline at 5 minutes of standing compared to 1 minute of standing ($p=0.017$; Table 8).

3.2.6 Ventilation & Oxygen Consumption

During standing, there was a statistically significant main effect of time on Rf ($p=0.033$; Table 8); however, pairwise comparisons did not reveal any significant differences between supine and any standing time point ($p>0.135$). Similarly, there were differences in the change in Rf from baseline across time ($p=0.017$; Table 8), but pairwise comparisons did not show any significant differences ($p>0.051$). There were no significant differences in absolute VO_2, relative VO_2, Tv, and V_E from supine to standing ($p>0.132$; Table 8). There was a significantly greater change in V_E from baseline after 3 minutes of standing compared to after 1 minute of standing ($p=0.010$; Table 8). There were no significant differences in the changes in absolute VO_2, relative VO_2, and Tv, from baseline throughout minutes 1, 3, 5, and 10 of standing ($p>0.272$).

Table 8. Cardiopulmonary hemodynamic responses to the invasive active stand test (n=14).

	Supine	Stand 1-min	Stand 3-mins	Stand 5-mins	Stand 10-mins	*p*-value
Hemodynamics						
HR (bpm)	61 ± 9	68 ± 11***	69 ± 12***	70 ± 13***	71 ± 12***	**<0.001**
ΔHR (bpm)	--	5 (3-12)	6 (2-16)	7 (2-15)	9 (4-12)	0.374
SBP (mmHg)	133 ± 17	137 ± 21	135 ± 20	132 ± 20	129 ± 17*	**0.013**
ΔSBP (mmHg)	--	5 ± 10	3 ± 10	0 ± 8	-3 ± 7[a,b]	**0.006**
DBP (mmHg)	78 ± 10	79 ± 9	81 ± 10	80 ± 10	78 ± 9	0.434
ΔDBP (mmHg)	--	1 ± 7	2 ± 8	2 ± 7	0 ± 6	0.231
MAP (mmHg)	98 ± 14	100 ± 12	100 ± 12	100 ± 13	97 ± 12	0.180
ΔMAP (mmHg)	--	2 ± 7.3	3 ± 8	2 ± 7	0 ± 6	0.074
Cardiac Output Measurements						
CO_{TD} (L/min)	6.1 ± 1.5	--	--	5.0 ± 1.2***	--	**<0.001**
ΔCO_{TD} (L/min)	--	--	--	-1.2 ± 0.9	--	--
CO_{DF} (L/min)	5.5 (4.6-7.3)	3.7 (3.5-4.8)**	3.9 (3.3-4.7)***	3.8 (3.2-4.7)**	4.0 (3.5-4.9)**	**<0.001**
ΔCO_{Fick} (L/min)	--	-1.5 (-2.3- -0.7)	-1.5 (-2.4- -1.2)	-1.5 (-2.7- -0.9)	-1.8 (-2.5- -1.0)	0.557
SV_{TD} (mL)	102 ± 25	--	--	71 ± 16***	--	**<0.001**
ΔSV_{TD} (mL)	--	--	--	-32 ± 19	--	--
SV_{Fick} (mL)	90 (74-107)	60 (49-75)*	54 (41-64)***	55 (46-67)**	54 (48-68)***	**<0.001**
ΔSV_{Fick} (mL)	--	-37 (-45- -6)	-34 (-50- -29)	-41 (-49- -22)	-34 (-50- -22)	0.520
Pulmonary Blood Pressures						
RaP (mmHg)	5 ± 3	1 ± 2***	1 ± 2***	1 ± 1***	0 ± 2***	**<0.001**
ΔRaP (mmHg)	--	-6 ± 3	-6 ± 3	-6 ± 3	-6 ± 3	0.750
RVSP (mmHg)	28 ± 4	23 ± 5	22 ± 4*	21 ± 5***	21 ± 5***	**<0.001**
ΔRVSP (mmHg)	--	-5 ± 4	-7 ± 4[a]	-7 ± 4[a]	-7 ± 4[a]	**<0.001**
RVDP (mmHg)	2 (0-4)	-1 (-5- -2)	-2 (-5- -1)*	-4 (-5- -2)**	-4 (-5- 1)***	**<0.001**
ΔRVDP (mmHg)	--	-3 ± 3	-4 ± 3	-4 ± 3[a]	-5 ± 3[a]	**0.009**
RVEDP (mmHg)	8 ± 3	2 ± 5*	1 ± 4**	1 ± 4***	0 ± 4***	**<0.001**
ΔRVEDP (mmHg)	--	-8 (-10- -4)	-8 (-10- -5)	-8 (-10- -5)	-8 (-11- -6)	0.352
PASP (mmHg)	25 ± 4	17 ± 3***	16 ± 3***	15 ± 3***	15 ± 3***	**0.011**
ΔPASP (mmHg)	--	-9 (-11- -7)	-9 (-13- -7)	-10 (-13- -8)	-11 (-14- -7)[a]	**0.012**

PADP (mmHg)	10 (9-11)	6 (4-8)*	6 (3-8)**	6 (2-7)**	6 (2-8)***	**<0.001**
ΔPADP (mmHg)	--	-4 (-7- -3)	-5 (-7- -4)	-6 (-8- -4)	-5 (-8- -4)	0.380
mPAP (mmHg)	17 ± 3	11 ± 2***	10 ± 3***	10 ± 3***	9 ± 3***	**0.011**
ΔmPAP (mmHg)	--	-6 ± 3	-7 ± 3	-7 ± 3	-8 ± 3	**0.013**
PAWP (mmHg)	11 ± 2	3 ± 3*	2 ± 2***	3 ± 2**	2 ± 2***	**<0.001**
ΔPAWP (mmHg)	--	-9 (-11- -7)	-9 (-11- -8)	-9 (-11- -7)	-9 (-12- -8)[a]	**0.007**
Blood Oximetry						
SaO_2 (%)	99 (97-100)	100 (98-100)	99 (98-100)	99 (98-100)	99 (98-100)	0.996
ΔSaO_2 (%)	--	1 (0-2)	0 (0-1)	1 (0-1)	0 (0-1)	**0.021**
CaO_2 (mL/dL)	19 (17-20)	19 (18-20)	19 (18-20)	19 (18-20)	19 (18-20)	1.000
ΔCaO_2 (mL/dL)	--	0.18 (0.00-0.32)	0.00 (0.00-0.20)	0.00 (0.00-0.22)	0.00 (0.00-0.22)	**0.014**
SvO_2 (%)	73 (70-76)	64 (59-70)***	66 (61-68)***	64 (60-67)***	64 (58-66)***	**<0.001**
ΔSvO_2 (%)	--	-8 (-14- -6)	-9 (-11- -7)	-9 (-12- -7)	-10 (-13- -7)	0.733
CvO_2 (mL/dL)	14 (12-15)	12 (11-14)**	13 (11-14)***	12 (11-13)***	12 (11-13)***	**<0.001**
ΔCvO_2 (mL/dL)	--	-1.6 (-2.9- -1.1)	-1.7 (-2.5- -1.3)	-1.7 (-2.7- -1.3)	-1.9 (-2.7- -1.3)	0.733
Peripheral Muscle Oxygenation						
SmO_2 (%)	70 ± 16	61 ± 19***	57 ± 20***	56 ± 20***	55 ± 22***	**<0.001**
ΔSmO_2 (%)	--	-8 (-14- -4)	-15 (-19- -7)	-16 (-20- -8)[a]	-17 (-22- -7)	**0.032**
THb (au)	12 (12-13)	12 (12-13)	12 (12-13)	12 (12-13)*	12 (12-13)*[,a]	**<0.001**
ΔTHb (au)	--	0.12 ± 0.23	0.18 ± 0.26	0.23 ± 0.27[a,b]	0.28 ± 0.33[a,b]	**<0.001**
O_2Hb (au)	8.50 ± 1.7	7.4 ± 2.0	6.9 ± 2.1***	6.8 ± 2.2***	6.7 ± 2.4***	**<0.001**
ΔO_2Hb (au)	--	-0.9 (-1.7- -0.5)	-1.4 (-2.2- -0.9)	-1.8 (-2.3- -1.0)[a]	-1.9 (-2.5- -0.9)	**0.032**
HHb (au)	3.60 ± 2.1	4.8 ± 2.4***	5.3 ± 2.6***	5.5 ± 2.6***[,a]	5.7 ± 2.9***[,a]	**<0.001**
ΔHHb (au)	--	1.1 (0.5-1.9)	1.9 (0.9-2.4)	2.2 (1.0-2.6)[a]	2.3 (0.9-3.0)	**0.017**
Ventilation & Oxygen Consumption						
VO_2 (mL/min)	263 (229-294)	267 (228-327)	253 (223-289)	255 (236-298)	263 (244-298)	0.298
ΔVO_2 (mL/min)	--	20 (-34-47)	-20 (-35-5)	5 (-16-19)	2 (-27-23)	0.272
VO_2 (mL/kg/min)	3.7 (3.3-4.0)	3.8 (3.1-4.5)	3.4 (2.7-4.2)	3.6 (3.2-4.1)	3.9 (3.1-4.2)	0.272
ΔVO_2 (mL/kg/min)	--	0.23 (-0.49-0.75)	-0.26 (-0.46-0.06)	0.06 (-0.31-0.25)	0.00 (-0.33-0.33)	0.272
Tv (L)	0.54 (0.46-0.66)	0.62 (0.51-0.71)	0.63 (0.49-0.71)	0.62 (0.51-0.71)	0.59 (0.47-0.71)	0.425
ΔTv (L)	--	0.07 (-0.01-0.14)	0.09 (-0.04 -0.12)	0.09 (-0.03 -0.14)	0.01 (-0.06 -0.14)	0.614
Rf (breath/min)	17 ± 3	16 ± 3	14 ± 3	14 ± 3	16 ± 3	**0.033**

ΔRf (breath/min)	--	-1.0 ± 4.2	-2.3 ± 3.6	-1.8 ± 3.5	-1.0 ± 3.1	**0.017**
V_E (L/min)	8.7 (7.4-10.1)	9.6 (7.8-11.3)	8.5 (6.7-9.4)	8.7 (7.5-9.4)	8.7 (7.4-9.9)	0.132
ΔV_E (L/min)	--	0.94 ± 2.18	-0.50 ± 1.39[a]	-0.17 ± 0.81	-0.04 ± 1.10	**0.010**

Normal data are be reported as mean ± SD and non-normal data as median (interquartile range). p-values are from one-way repeated measures ANOVA. Tukey post-hoc tests vs. supine baseline ($p<0.05$*, $p<0.01$**, $p<0.001$***). Δ values present Stand– Supine. au, arbitrary units; CaO_2, arterial oxygen content; CO_{DF}, Direct Fick cardiac output; CO_{TD}, thermodilution cardiac output; CvO_2, mixed-venous oxygen content; DBP, diastolic blood pressure; HHb, relative deoxyhemoglobin; HR, heart rate; MAP, mean arterial blood pressure; mPAP, mean pulmonary artery pressure; O_2Hb, relative oxyhemoglobin; PADP, pulmonary artery diastolic pressure; PASP, pulmonary artery systolic pressure; PAWP, pulmonary arterial wedge pressure; RaP, right atrial pressure; Rf, respiratory frequency; RVDP, right ventricular diastolic pressure; RVEDP, right ventricular end diastolic pressure; RVSP, right ventricular systolic pressure; SaO_2, arterial oxygen saturation; SBP, systolic blood pressure; SmO_2, vastus lateralis muscle oxygenation; SV_{DF}, Direct Fick stroke volume; SV_{TD}, thermodilution stroke volume; SvO_2 mixed-venous oxygen saturation; THb, relative total hemoglobin; Tv, tidal volume; V_E, minute ventilation; VO_2, oxygen uptake. *a* indicates a significant difference from Stand 1-min. *b* indicates a significant difference from Stand 3-mins.

3.2.7 Comparison of the Change of Mean Cerebral Blood Velocity to the Changes of Cardiopulmonary Hemodynamic Measurements

The changes of each cardiopulmonary hemodynamic measurement in predicting change in MCAv were examined. The change in mean MCAv with standing was not associated with the changes of any central hemodynamic variables (ΔHR, ΔSBP, ΔDBP, ΔMAP; $p>0.230$; Table 9). Changes in thermodilution and direct Fick derived CO and SV also did not demonstrate significant relationships with change in mean MCAv ($p>0.651$; Table 9). Regarding pulmonary and cardiac filling blood pressures, the change in mean MCAv demonstrated a strong negative relationship with change in RSVP ($r=-0.669$, $p<0.034$; Table 9: Fig. 9) and a strong negative relationship with change in PAWP ($r=-0.627$, $p<0.039$; Table 9: Fig. 10). There were no associations found between change in mean MCAv and changes in any blood oximetry or peripheral muscle oxygenation variable (ΔSaO_2, ΔCaO_2, ΔSvO_2, ΔCvO_2, ΔSmO_2, ΔTHb, ΔO_2Hb, ΔHHb; $p>0.145$; Table 9). There was a negative correlation between the changes in mean MCAv and absolute VO_2 ($r=-0.660$, $p=0.019$; Table 9; Fig. 11). Of note, there were three additional trends what were observed. The change in RVEDP trended towards a negative correlation ($r=-0.611$, $p=0.60$; Table 9), the change in mPAP trended towards a negative correlation ($r=-0.584$, $p<0.059$; Table 9), and the change in normalized VO_2 trended towards a negative correlation ($r=-0.556$, $p=0.060$; Table 9) with the change in mean MCAv. When these trends were subsequently forced into a stepwise forward regression, no significant relationships were found ($p>0.339$).

Table 9. Linear regression analysis of the change in mean MCAv vs the changes in cardiopulmonary hemodynamic measures during the invasive active stand test.

Independent Variable	Dependent Variables	r	R^2	*p*-value
	Hemodynamics			
ΔMean MCA (cm/s)	ΔHR (bpm)	0.098	0.010	0.762
	ΔSBP (mmHg)	-0.375	0.140	0.230
	ΔDBP (mmHg)	0.079	0.006	0.808
	ΔMAP (mmHg)	-0.077	0.006	0.811
	Cardiac Output Measurements			
	ΔCO_{TD} (L/min)	0.006	0.000	0.986
	ΔCO_{DF} (L/min)	-0.154	0.023	0.651
	ΔSV_{TD} (mL)	0.055	0.003	0.873
	ΔSV_{DF} (mL)	0.000	0.000	0.998
	Pulmonary Blood Pressures			
	ΔRaP (mmHg)	-0.455	0.207	0.160
	ΔRVSP (mmHg)	-0.669	0.448	**0.034**
	ΔRVDP (mmHg)	-0.493	0.243	0.148
	ΔRVEDP (mmHg)	-0.611	0.374	0.060
	ΔPASP (mmHg)	-0.303	0.092	0.364
	ΔPADP (mmHg)	-0.504	0.254	0.114
	ΔmPAP (mmHg)	-0.584	0.341	0.059
	ΔPAWP (mmHg)	-0.627	0.393	**0.039**
	Blood Oximetry			
	ΔSaO_2 (%)	0.470	0.221	0.145
	ΔCaO_2 (mL/dL)	0.359	0.129	0.279
	ΔSvO_2 (%)	0.021	0.000	0.951
	ΔCvO_2 (mL/dL)	0.102	0.010	0.766

	Peripheral Muscle Oxygenation			
	ΔSmO_2 (%)	0.277	0.077	0.383
	ΔTHb (au)	-0.185	0.034	0.564
	ΔO_2Hb (au)	0.300	0.090	0.343
	ΔHHb (au)	-0.337	0.114	0.284
	Ventilation & Oxygen Consumption			
	ΔVO_2 (mL/min)	-0.660	0.436	**0.019**
	ΔVO_2 (mL/kg/min)	-0.556	0.310	0.060
	ΔTv (L)	0.052	0.003	0.873
	ΔRf (breath/min)	-0.370	0.137	0.236
	ΔV_E (L/min)	-0.523	0.273	0.081

au, arbitrary units; CaO_2, arterial oxygen content; CO_{DF}, Direct Fick cardiac output; CO_{TD}, thermodilution cardiac output; CvO_2, mixed-venous oxygen content; DBP, diastolic blood pressure; HHb, relative deoxyhemoglobin; HR, heart rate; MAP, mean arterial blood pressure; mPAP, mean pulmonary artery pressure; O_2Hb, relative oxyhemoglobin; PADP, pulmonary artery diastolic pressure; PASP, pulmonary artery systolic pressure; PAWP, pulmonary arterial wedge pressure; RaP, right atrial pressure; Rf, respiratory frequency; RVDP, right ventricular diastolic pressure; RVEDP, right ventricular end diastolic pressure; RVSP, right ventricular systolic pressure; SaO_2, arterial oxygen saturation; SBP, systolic blood pressure; SmO_2, vastus lateralis muscle oxygenation; SV_{DF}, Direct Fick stroke volume; SV_{TD}, thermodilution stroke volume; SvO_2 mixed-venous oxygen saturation; THb, relative total hemoglobin; Tv, tidal volume; V_E, minute ventilation; VO_2, oxygen uptake.

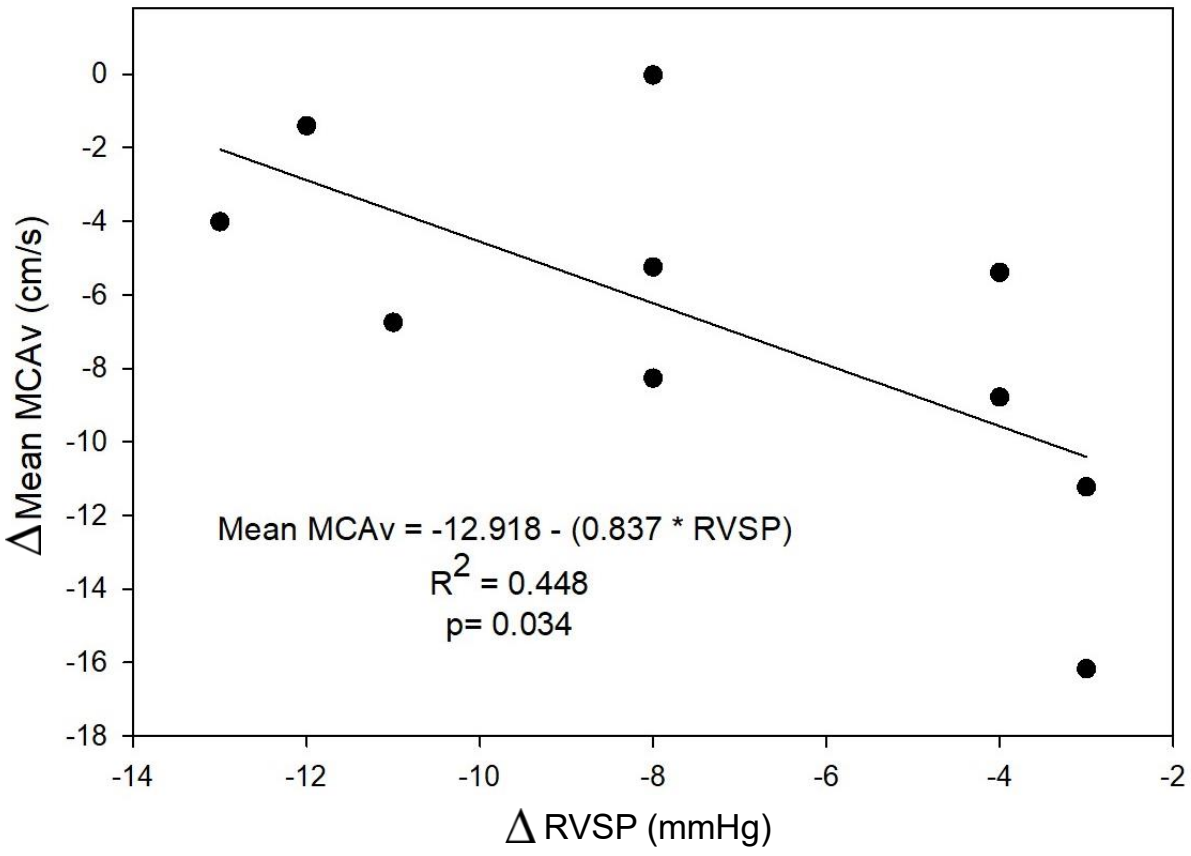

Figure 10. Association between changes in right ventricular systolic pressure (RVSP) and mean middle cerebral artery velocity (MCAv) due to standing.

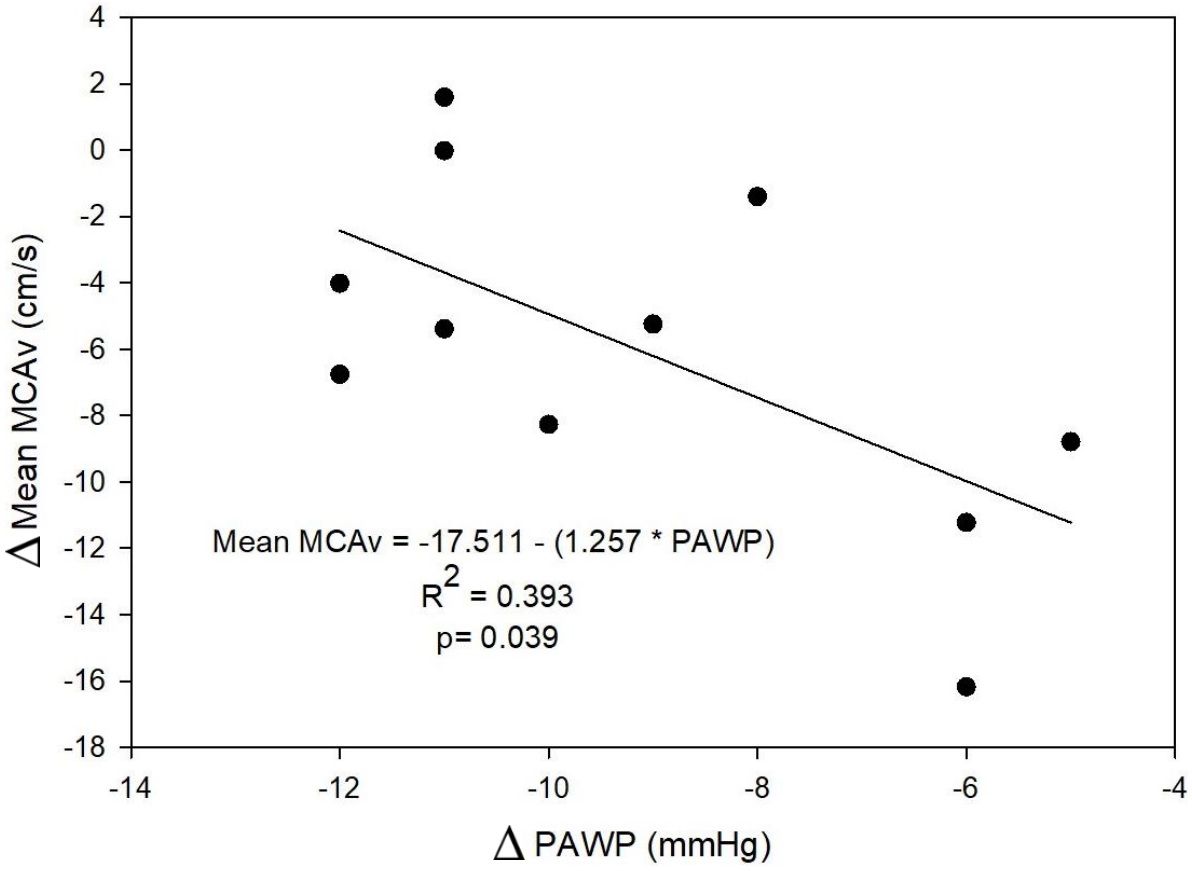

Figure 11. Association between changes in pulmonary artery wedge pressure (PAWP) and mean middle cerebral artery velocity (MCAv) due to standing.

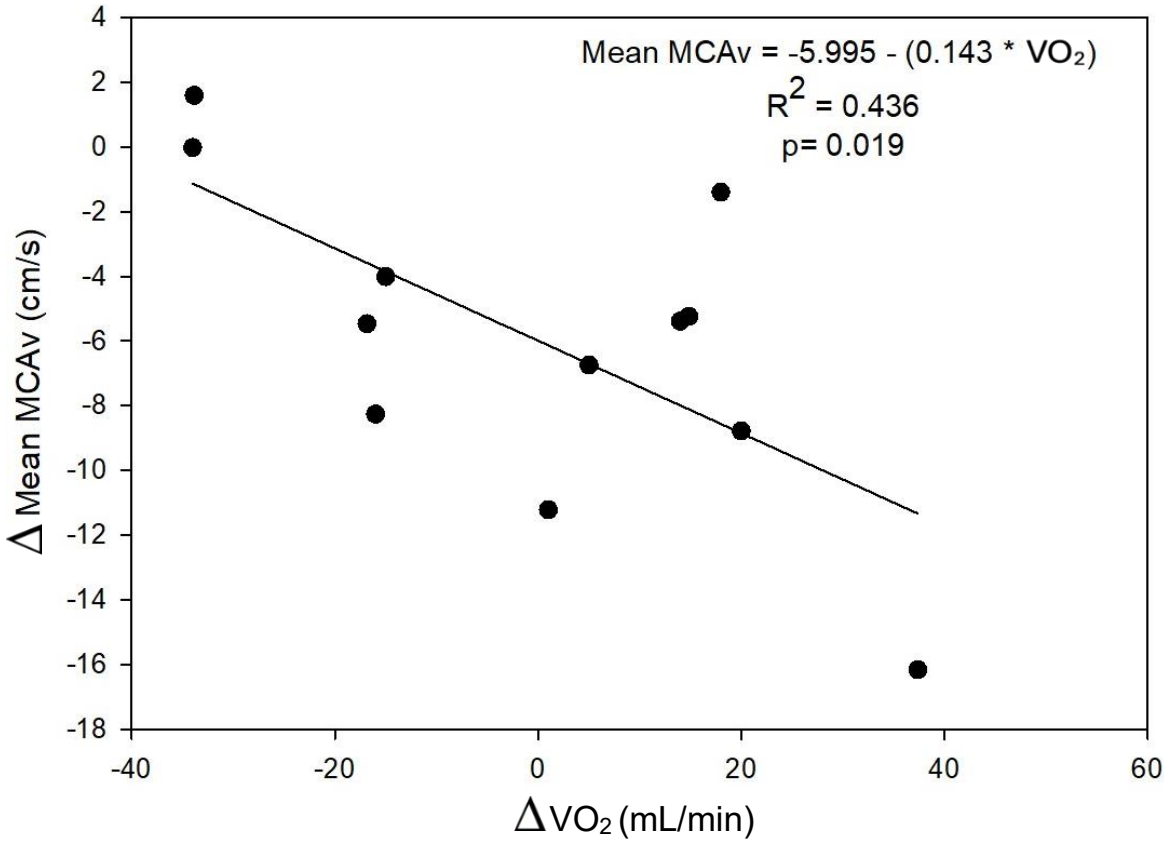

Figure 12. Association between changes in absolute oxygen uptake (VO_2) and mean middle cerebral artery velocity (MCAv) due to standing.

Chapter 4: Discussion

4.1 Summary

The current study primarily investigated the relationship between the change in MCAv and changes in invasive CO measurements during an AST in a healthy population to investigate the extent to which alterations in CO may contribute to CBF during standing. To our knowledge, there are no previous studies examining the association between invasive CO and MCAv during orthostatic stress in a healthy population. By directly comparing invasive CO measurements with MCAv responses, we have provided further insight into the cardiovascular and cerebrovascular mechanisms that occur during postural change. Additionally, we evaluated changes in cerebral resistance, cerebral autoregulation, autonomic function, and cardiopulmonary parameters in relation to the change in MCAv to explore any potential alternate mechanisms underlying cerebral perfusion during orthostatic stress and to establish a healthy physiological baseline for future comparisons with individuals with OI such as POTS or OH. Overall, our findings suggest that greater CVRi leads to reduced MCAv which in turn leads to reduced HF cerebral autoregulation and reduced VR from the brain and thus less cardiac filling during orthostatic stress.

We hypothesized that:

1. During standing, reductions in CO would drive reduced MCAv in a young healthy population of men and women—This hypothesis was rejected.
2. Due to previous evidence finding that parasympathetic nervous activity causes cerebral vasodilation (Conway et al., 2006), we hypothesized that parasympathetic withdrawal during upright posture would be a predictor of reductions in MCAv—This hypothesis was rejected.
3. Due to previous findings that there are no significant changes of dynamic autoregulation indices while upright (Robertson et al., 2020), we hypothesized that dynamic autoregulation would not predict reductions in MCAv during stand—This hypothesis was rejected.

In summary, all three of our initial hypotheses were rejected. Collectively, our findings suggest that the determinants of MCAv during standing are more complex than initially proposed and are not explained by CO or cardiac parasympathetic withdrawal. The present findings reveal a more

integrated model in which both cerebral and cardiopulmonary mechanisms contribute to the cerebral blood velocity responses.

4.2 Associations Between Changes in Cardiac Output and Cerebral Blood Velocity During Orthostasis

When the relationship between changes in CO and MCAv due to standing was examined, CO was not identified as a significant determinant of cerebral blood velocity. Past studies investigated concurrent observations of CO and MCAv in young healthy adults under conditions of reduced central blood volume, induced by standing (Edgell et al., 2012; van Lieshout et al., 2001) or lower body negative pressure (Ogoh et al., 2005), and reported decreases in both CO and MCAv ; however, none examined the direct relationship between these variables. Furthermore, these investigations relied on only non-invasive estimates of CO, including Fick-derived CO (van Lieshout et al., 2001), finger blood pressure pulse contour analysis (Edgell et al., 2012) and the acetylene re-breathing technique (Ogoh et al., 2005). In our study, we utilized two methods to derive CO: thermodilution CO (invasive measurement) and direct Fick derived CO (non-invasive measurement) and we similarly observed reductions in both CO and MCAv during orthostatic stress. Building on these previous findings, the current study extended this work by directly examining the relationship between changes in CO and MCAv during standing. Despite significant reductions in both CO and MCAv from supine to standing, CO was not identified as a significant determinant of MCAv during standing. Similarly, a study done by Garrett et al. (2017) using pulse contour analysis to calculate CO also did not reveal a relationship between CO and MCAv when comparing between supine and upright sitting.

4.3 Associations Between Changes in Cardiac Measures and Cerebral Blood Velocity During Orthostasis

To our knowledge, the present study is the first to directly measure the changes in right atrial, ventricular, pulmonary, and PAWP during a 10-minute AST in a healthy population. Interestingly, the change in MCAv was negatively associated with changes in cardiac filling pressures, assessed through measurements of PAWP and RVSP. With standing, greater reductions in PAWP were associated with a smaller reduction in MCAv. Similarly, there was a negative

correlation between the changes in RVSP and MCAv. These findings suggest that less cardiac filling is associated with preserving brain blood velocity while standing. Interestingly, this influence of cardiac filling pressures was observed without a concurrent influence of SV or CO, suggesting a potential influence of the CPBR. The CPBR includes specialized mechanoreceptors, located in the heart, pulmonary blood vessels, and vena cava (Donald & Shepherd, 1978; Uchida, 1975), which influence the efferent sympathetic nerve activity by detecting and responding to changes in central blood volume and central venous pressure (i.e. cardiac filling pressure) (Donald & Shepherd, 1978; reviewed in Katayama & Ogoh, 2025).

During orthostatic stress, reductions in central blood volume and cardiac filling pressures would unload the cardiopulmonary stretch receptors, resulting in an increase in sympathetic outflow and parasympathetic withdrawal (reviewed in Katayama & Ogoh, 2025; Mark & Mancia, 1983). While we did not find a relationship between the change in MCAv during standing and changes in cardiac autonomic function (discussed below), we suggest that changes to cerebral autonomic function are still relevant to consider. Indeed, it is important to highlight that cardiac autonomic regulation does not directly equate to autonomic control of the cerebral vasculature. Anatomical differences, adrenoreceptor subtypes, distribution, sensitivity, and density, provide evidence that measures of the peripheral sympathetic nerve activity cannot be generalized to cerebral nerve activity (reviewed in Koep et al., 2022).

4.4 Associations Between Changes in Autonomic Function and Cerebral Blood Velocity During Orthostasis

As cerebral autonomic function cannot be assessed in humans, HRV and cBRS analysis were performed as indices of cardiac autonomic function. Due to standing, our data demonstrated significant reductions in RR mean, SDRR, the HF component of HRV, Poincaré SD2 and cBRS. These findings were expected and align with previous studies that found cardiac parasympathetic withdrawal in response to posture change in healthy adults (Abidi et al., 2017; Robertson et al., 2020). However, in the current study we uniquely assessed the relationship between changing indices of cardiac autonomic function and MCAv during orthostatic stress. Contrary to our hypothesis, cardiac parasympathetic withdrawal was not predictive of reductions in MCAv during standing. However, as noted earlier, cardiac autonomic function does not

necessarily equate to cerebral autonomic function. Interestingly, previous animal work done by Morita et al. (1994) found that bilateral parasympathetic denervation reduced cerebral autoregulation, highlighting the importance of parasympathetic control of CBF. Similarly, work done by Gelpi et al. (2021) found a strong negative correlation between cerebral autoregulation index and markers of vagal modulation (HF power), and a positive correlation with indices of sympathetic modulation (LF power) in a supine position in young healthy adults (Gelpi et al., 2021). Together, these studies suggest that changes in cerebral autonomic control could potentially influence cerebral autoregulation.

4.5 Associations Between Changes in Cerebral Autoregulation and Cerebral Blood Velocity During Orthostasis

As expected, changes in systolic and diastolic MCAv were positively associated with the change in mean MCAv due to standing. Similarly, the change in MCAv was negatively associated with the change in CVRi (the quotient of CPP/MCAv), a measure of static cerebral autoregulation, such that higher resistance was associated with reduced cerebral blood velocity. This indicates that steady-state cerebrovascular resistance plays an important role in modulating cerebral perfusion during orthostatic stress. This interpretation is supported by previous work that demonstrated the integral role of CVR indices in predicting cerebral perfusion across the adult lifespan (Tomoto et al., 2023). Additionally, previously conducted tilt studies (Blaber et al., 2001; Serrador & Freeman, 2017) demonstrated the same relationship, where increases in CVR when upright were associated with greater reductions in CBF. Thus, the increased CVRi observed in the current study could be the driving factor behind the reduction of MCAv during standing.

Contrary to our hypothesis, dynamic autoregulation was in fact a significant determinant of changes in MCAv during standing. Specifically, the HF phase of cerebral autoregulation was found to have a positive correlation with changes in MCAv where a greater reduction of HF phase, hence a greater reduction of autoregulation, was associated with greater reductions in MCAv. LF and VLF ranges are more driven by a combination of autonomic vascular tone, cellular, and myogenic control mechanisms (reviewed in Vesoulis & Mathur, 2017). In contrast, the HF fluctuations are largely driven by the heart rate and respiratory cycle and therefore reflect

passive vascular properties and/or volume rather than active vascular control (Reehal et al., 2021; reviewed in Vesoulis & Mathur, 2017).

Previous studies investigated dynamic cerebral autoregulation in healthy young adults when comparing supine to 90° head-up tilt (Gelinas et al., 2012) or supine to sitting (Garrett et al., 2017). Gelinas and colleagues (2012) used a head-up tilt protocol (10 minutes supine followed by 10 minutes upright tilt at 90°) and reported increases in BP power (total power and LF power), increased coherence (VLF and LF ranges), decreased gain (LF band), and no significant changes in HF band with tilt. We also observed increased BP power (LF band), increased coherence (VLF frequency band), and no significant changes in HF band from supine to standing. Garret et al. (2017) used a sitting protocol (5 minutes supine, 5 minutes sitting up) to investigate CBF and autoregulation parameters with posture change and similarly found increased BP power in LF and VLF frequencies, and reduced gain in all frequencies (VLF, LF, HF) (Garrett et al., 2017) in the seated position. Similarly, we also found increased BP power in the LF frequency band and decreased gain (VLF band). Together, all of these studies reveal attenuated transfer function gain while upright, indicating better dynamic autoregulation of CBF. In contrast, a separate study looking at cerebrovascular responses to an orthostatic tilt test (5 minutes supine followed by only 5 minutes upright tilt at 70°), observed increased MCAv power and increased coherence within the LF frequency band, with no significant changes in HF and VLF ranges with tilt (Andrew. Robertson et al., 2020). Overall, Robertson et al. (2020) did not find an effect of tilt on dynamic cerebral autoregulation parameters. Discrepancies in results and findings from these studies may be explained by differences in methodological approaches, including the magnitude and duration of the postural challenge (sitting versus head-up tilt versus active standing). These methodological variations may influence the magnitude of cerebrovascular hemodynamics, which have been shown to differ between sitting and standing (Edgell et al., 2012), which in turn may affect autoregulation. While all these studies explored the effect of postural changes on cerebral autoregulation, the extent to which changes in dynamic autoregulation impacted the change in MCAv was not investigated.

Since we observed that a reduction in HF phase was positively associate with a reduction in MCAv, in the absence of a relationship with VLF or LF phase, we suggest that a passive relationship between cerebral volume and dynamic autoregulation exists during standing.

4.6 Associations Between Changes in Ventilation and Cerebral Blood Velocity During Orthostasis

Previous studies have investigated ventilatory responses to orthostatic stress with head-up tilt (Chang et al., 2005) or active standing protocols (Chang et al., 2005; van Lieshout et al., 2001). For the head-up tilt test (10 minutes supine followed by 5 minutes of upright tilt at 70°), Chang et al. (2005) reported increased V_E and no changes in Rf in healthy young male participants. The same study demonstrated similar results with unsupported standing (10 minutes supine followed by 5 minutes of standing): increased V_E and no significant changes in Rf with standing (Chang et al., 2005). Similarly, van Lieshout et al. (2001) reported increased V_E in healthy adults with standing. Despite methodological differences, we also observed greater V_E without a change in Rf with standing. Specifically, Chang et al. (2005) used a respiratory mechanics monitor (Ventrak, Model 1550 Novametrix Medical Systems Inc. Wallingfrod, CT, USA) and van Lieshout et al. (2001) used a metabolic cart (MedGraphics CPX/D) for their ventilatory analysis.

Surprisingly, we found a negative association between the change in absolute oxygen consumption and the change in MCAv during standing. This relationship suggests that increased oxygen consumption is associated with greater reductions in brain blood velocity; however, in the current study design, we cannot determine which change precedes the other. The reductions in MCAv may impair postural stability, eliciting greater skeletal muscle activation to maintain upright posture. Increased skeletal muscle pump activity may subsequently augment venous return and cardiac filling as a compensatory response to maintain arterial pressure and cerebral perfusion. Therefore, we suggest that in the absence of clear changes in V_E of Rf, the relationship between VO_2 and MCAv is attributable to increased skeletal muscle activity and muscle pump engagement. Future studies should consider assessing muscle pump activity in postural studies using electromyography on postural muscles and/or force plate analysis during standing.

4.7 Limitations and Future Directions

This study was limited by its small sample size, potentially affecting the generalizability of the findings, due to limited sex, gender, and ethnicity in the sample. Additionally, achieving statistical significance is more challenging in smaller sample sizes. For example, several trends

were observed in the current study that may have reached statistical significance with a larger sample size. Future studies should aim to include a larger sample size to improve statistical power (which ranged from 0.025 to 0.999 in the current study), with a balanced representation of biological sex and a broader range of participant characteristics, including age, ethnicity, physical activity level, and body composition, to explore inter-individual variability.

In the non-invasive protocol, brachial BP was measured using an oscillometric cuff (Phillips IntelliVue MP5, Philips Healthcare, Canada), a commonly used clinical device for estimating systolic and diastolic blood pressure. This technique was used to calibrate the ongoing beat-to-beat BP device to ensure accuracy. However, compared with auscultatory methods (e.g., manual sphygmomanometry or Tango+), oscillometric devices demonstrate less agreement with intra-arterial measurements (Babadağ & Zaybak, 2021). Further, intracardiac pressure transducers were zeroed to the phlebostatic axis at the level of the fourth intercostal space along the midaxillary line to approximate right atrial height. However, this external reference does not account for postural shifts in thoracic anatomy (Beillas et al., 2009) nor variability between people. Consequently, differing downward displacement of the heart during standing may have resulted in under or overestimation of intracardiac pressure measurements due to hydrostatic differences between the transducer and the right atrium. This limitation may be further influenced by sex-related differences in thoracic and chest morphology, which may affect the magnitude of cardiac displacement during postural changes.

A limitation of the present study is the lack of normalization of CO and SV to BSA, particularly given the inclusion of a mixed-sex cohort. Absolute values of SV and CO are known to differ between males and females, largely due to the differences in body size and cardiac dimensions; with males generally having larger body surface areas, CO, and SV than females (reviewed in St. Pierre et al., 2022). As such, males would be expected to exhibit larger absolute reductions in SV and CO during orthostatic stress because their baseline values are greater (Rutkowski et al., 2020; reviewed in St. Pierre et al., 2022). Consequently, the use of non-indexed values may have introduced a bias, whereby sex-related differences in body size may have obscured true physiological responses to standing. This may have limited the ability to detect significant relationships between changes in CO and SV and changes in MCAv. Future studies should normalize CO and SV measures to BSA to account for inter-individual differences

in body size and cardiac dimensions, thereby improving the assessment of cardiovascular responses to orthostatic stress.

We further acknowledge that the use of HRV as an index of autonomic balance is limited, and that this measure of cardiac autonomic modulation does not necessarily reflect cerebral, regional or systemic autonomic function. To address this limitation, we would recommend future studies to investigate more direct measures of ANS (e.g. peroneal microneurography to assess muscle sympathetic nerve activity). However, we acknowledge that these measures still may not adequately assess autonomic influence of the cerebral vasculature. Additionally, future studies may benefit from animal models or pharmaceutical interventions when assessing autonomic function and CBF. In particular, pharmacological manipulation of autonomic control using ganglionic blockade or anticholinergic agents could help isolate the contribution of sympathetic and parasympathetic pathways to CBF regulation (Claassen et al., 2021). These interventions, combined with measurements of cerebral hemodynamics using TCD or MRI, could provide a more accurate assessment of cerebrovascular responses under controlled autonomic conditions.

During the invasive Visit 2 protocol, the arm into which the right heart catheter was inserted was not used for support by the participant during the transition to standing, which extended the time required to achieve an upright posture (on average ~15-20 seconds in total), compared to the transition time during Visit 1 (on average ~7 seconds in total) . Additionally, participants frequently paused in a seated position during the Visit 2 protocol (~5-10 seconds) when transitioning from supine to standing, which resulted in a prolonged transition. This brief intermediate seated position may have allowed a more gradual redistribution of thoracic blood volume and earlier activation of compensatory hemodynamic mechanisms, potentially influencing the timing of their orthostatic responses. Future studies should aim to minimize the duration of the sit-to-stand transition or implement a more standardized transition protocol to better capture the physiological responses to orthostatic stress.

For practical reasons, neither the partial pressure of CO_2 dissolved in blood nor end-tidal CO_2 were measured. With standing, arterial and end-tidal CO_2 are expected to decrease (Abidi et al., 2017; Chang et al., 2005; Edgell et al., 2012; Andrew. Robertson et al., 2020; Serrador et al., 2006) potentially due to increases in V_E. CBF has been found to be very sensitive to changes in CO_2 (Battisti-Charbonney et al., 2011; Edgell et al., 2012; Panerai et al., 2019; Robertson et al.,

2020), where reductions in CO_2 drive reductions in brain blood flow. Since we found an association between oxygen consumption and the change in MCAv in this study, there is a likelihood that there would also be a relationship between the change in MCAv and the change in arterial CO_2. Future studies should consider incorporating measurements of arterial or end-tidal CO_2 during orthostatic testing to further characterize the contribution of CO_2 to changes in CBF.

Future work should extend to clinical populations characterized by OI, including POTS and OH. Given our findings highlighting the importance of cardiac filling pressures, their assessment may be particularly informative in these populations. For example, people with POTS have reduced cardiac size and central blood volume (Fu et al., 2010) which may alter the CPBR. Indeed, POTS patients have been found to have exaggerated MSNA responses to baroreflex challenges when compared with healthy individuals. Investigating cardiac filling pressures, cerebral hemodynamic, autoregulatory, and ventilatory responses in these populations may improve understanding of the pathophysiological mechanisms underlying OI and help identify targets for clinical intervention. Lastly, future studies should examine the effects of interventions targeting dynamic cerebral autoregulation and cardiac filling pressures. Potential interventions may include exercise training, volume-expanding strategies (i.e. dietary sodium/fluid loading, lower-body compression garments), breathing training, and pharmacological interventions.

4.8 Conclusions

The current study primarily examined the relationship between the change in MCAv and changes in invasively measured CO during an AST in a healthy cohort. The change in MCAv was positively correlated with the change in autoregulatory HF phase and negatively correlated with the changes in cerebrovascular resistance, right ventricular systolic pressure, pulmonary artery wedge pressure, and absolute oxygen consumption. Overall, an increase in cerebrovascular resistance could be driving a reduction in cerebral flow during standing. In turn, this reduction of cerebral flow/volume could be driving the observed reductions in dynamic autoregulation and cerebral VR. The reduction in cerebral VR is the likely contributing factor to the observed reduced cardiac filling pressures. Subsequent to the reduced filling pressures, we expect that the

CPBRs would cause increased sympathetic and reduced parasympathetic activity in order to increase BP and thus preserve/increase brain blood flow.

References

Aaslid, R., Lindegaard, K. F., Sorteberg, W., & Nornes, H. (1989). Cerebral autoregulation dynamics in humans. *Stroke*, *20*(1), 45–52. https://doi.org/10.1161/01.STR.20.1.45

Aaslid, R., Markwalder, T. M., & Nornes, H. (1982). Noninvasive transcranial Doppler ultrasound recording of flow velocity in basal cerebral arteries. *Journal of Neurosurgery*, *57*(6), 769–774. https://doi.org/10.3171/jns.1982.57.6.0769

Abidi, S., Nili, M., Serna, S., Kim, S., Hazlett, C., & Edgell, H. (2017). Influence of sex, menstrual cycle, and oral contraceptives on cerebrovascular resistance and cardiorespiratory function during Valsalva or standing. *Journal of Applied Physiology*, *123*(2), 375–386. https://doi.org/10.1152/japplphysiol.00035.2017

Argueta, E. E., & Paniagua, D. (2019). Thermodilution Cardiac Output: A Concept Over 250 Years in the Making. *Cardiology in Review*, *27*(3), 138. https://doi.org/10.1097/CRD.0000000000000223

Armstead, W. M. (2016). Cerebral Blood Flow Autoregulation and Dysautoregulation. *Anesthesiology Clinics*, *34*(3), 465–477. https://doi.org/10.1016/j.anclin.2016.04.002

Babadağ, K., & Zaybak, A. (2021). Comparing Intra-Arterial, Auscultatory, and Oscillometric Measurement Methods for Arterial Blood Pressure. *Florence Nightingale Journal of Nursing*, *29*(2), 194–202. https://doi.org/10.5152/FNJN.2021.19103

Bartels, S. A., Stok, W. J., Bezemer, R., Boksem, R. J., van Goudoever, J., Cherpanath, T. G. V., van Lieshout, J. J., Westerhof, B. E., Karemaker, J. M., & Ince, C. (2011). Noninvasive cardiac output monitoring during exercise testing: Nexfin pulse contour analysis compared to an inert gas rebreathing method and respired gas analysis. *Journal of Clinical Monitoring and Computing*, *25*(5), 315–321. https://doi.org/10.1007/s10877-011-9310-4

Battisti-Charbonney, A., Fisher, J., & Duffin, J. (2011). The cerebrovascular response to carbon dioxide in humans. *The Journal of Physiology*, *589*(Pt 12), 3039–3048. https://doi.org/10.1113/jphysiol.2011.206052

Beillas, P., Lafon, Y., & Smith, F. W. (2009). The effects of posture and subject-to-subject variations on the position, shape and volume of abdominal and thoracic organs. *Stapp Car Crash Journal*, *53*, 127–154. https://doi.org/10.4271/2009-22-0005

Benarroch, E. E. (2008). The arterial baroreflex: Functional organization and involvement in neurologic disease. *Neurology*, *71*(21), 1733–1738. https://doi.org/10.1212/01.wnl.0000335246.93495.92

Blaber, A. P., Bondar, R. L., Moradshahi, P., Serrador, J. M., & Hughson, R. L. (2001). Inspiratory CO2 increases orthostatic tolerance during repeated tilt. *Aviation, Space, and Environmental Medicine*, *72*(11), 985–991.

Branthwaite, M. A., & Bradley, R. D. (1968). Measurement of cardiac output by thermal dilution in man. *Journal of Applied Physiology*, *24*(3), 434–438. https://doi.org/10.1152/jappl.1968.24.3.434

Breslin, D., Synnott, P., Byrne, C., Breslin, D., Synnott, P., & Byrne, C. (2023). Active Stand Testing for Identification of Postural Orthostatic Tachycardia Syndrome. *Cureus*, *15*. https://doi.org/10.7759/cureus.38281

Burton, A. C. (1951). On the Physical Equilibrium of Small Blood Vessels. *American Journal of Physiology-Legacy Content*, *164*(2), 319–329. https://doi.org/10.1152/ajplegacy.1951.164.2.319

Castro, R., Retamal, J., Hernández, G., Kattan, E., & Pinsky, M. R. (2026). Critical closing pressure in the circulation: Understanding the vascular waterfall phenomenon. *Journal of Critical Care*, *93*, 155485. https://doi.org/10.1016/j.jcrc.2026.155485

Chandra, A., Li, W. A., Stone, C. R., Geng, X., & Ding, Y. (2017). The cerebral circulation and cerebrovascular disease I: Anatomy. *Brain Circulation*, *3*(2), 45–56. https://doi.org/10.4103/bc.bc_10_17

Chang, A. T., Boots, R. J., Brown, M. G., Paratz, J. D., & Hodges, P. W. (2005). Ventilatory changes following head-up tilt and standing in healthy subjects. *European Journal of Applied Physiology*, *95*(5), 409–417. https://doi.org/10.1007/s00421-005-0019-2

Claassen, J. A. H. R., Thijssen, D. H. J., Panerai, R. B., & Faraci, F. M. (2021). Regulation of cerebral blood flow in humans: Physiology and clinical implications of autoregulation. *Physiological Reviews*, *101*(4), 1487–1559. https://doi.org/10.1152/physrev.00022.2020

Claassen, J. A., Meel-van den Abeelen, A. S., Simpson, D. M., & Panerai, R. B. (2016). Transfer function analysis of dynamic cerebral autoregulation: A white paper from the International Cerebral Autoregulation Research Network. *Journal of Cerebral Blood Flow & Metabolism*, *36*(4), 665–680. https://doi.org/10.1177/0271678X15626425

Clough, R. H., Panerai, R. B., Ladthavorlaphatt, K., Robinson, T. G., & Minhas, J. S. (2024). The complexity of cerebral blood flow regulation: The interaction of posture and vasomotor reactivity. *Journal of Applied Physiology*, *137*(4), 892–902. https://doi.org/10.1152/japplphysiol.00851.2023

Convertino, V. A. (1998). Gender differences in autonomic functions associated with blood pressure regulation. *The American Journal of Physiology*, *275*(6), R1909-1920. https://doi.org/10.1152/ajpregu.1998.275.6.R1909

Conway, C. R., Sheline, Y. I., Chibnall, J. T., George, M. S., Fletcher, J. W., & Mintun, M. A. (2006). Cerebral blood flow changes during vagus nerve stimulation for depression. *Psychiatry Research: Neuroimaging*, *146*(2), 179–184. https://doi.org/10.1016/j.pscychresns.2005.12.007

Deshpande, A., Zhang, L. Q., Balu, R., Yahyavi-Firouz-Abadi, N., Badjatia, N., Laksari, K., & Tahsili-Fahadan, P. (2025). Cerebrovascular morphology: Insights into normal variations, aging effects and disease implications. *Journal of Cerebral Blood Flow & Metabolism*, *45*(7), 1249–1264. https://doi.org/10.1177/0271678X251328537

Donald, D. E., & Shepherd, J. T. (1978). Reflexes from the heart and lungs: Physiological curiosities or important regulatory mechanisms. *Cardiovascular Research*, *12*(8), 446–469.

Donald, D. E., & Shepherd, J. T. (1980). Autonomic Regulation of the Peripheral Circulation. *Annual Review of Physiology*, *42*(1), 429–439. https://doi.org/10.1146/annurev.ph.42.030180.002241

Dremin, V., Volkov, M., Margaryants, N., Myalitsin, D., Rafailov, E., & Dunaev, A. (2025). Blood flow dynamics in the arterial and venous parts of the capillary. *Journal of Biomechanics*, *179*, 112482. https://doi.org/10.1016/j.jbiomech.2024.112482

DuBois, D., & DuBois, E. F. (1915). Fifth paper the measurement of the surface area of man. *Archives of Internal Medicine*, *5*(2), 868–881. https://doi.org/10.1001/archinte.1915.00070240077005

Edgell, H., Robertson, A. D., & Hughson, R. L. (2012). Hemodynamics and brain blood flow during posture change in younger women and postmenopausal women compared with

age-matched men. *Journal of Applied Physiology*, *112*(9), 1482–1493. https://doi.org/10.1152/japplphysiol.01204.2011

Euler, U. S. (1948). Identification of the Sympathominetic Ergone in Adrenergic Nerves of Cattle (Sympathin N) with Laevo-Noradrenaline. *Acta Physiologica Scandinavica*, *16*, 63–74. https://doi.org/10.1111/j.1748-1716.1948.tb00526.x

Fantini, S., Sassaroli, A., Tgavalekos, K. T., & Kornbluth, J. (2016). Cerebral blood flow and autoregulation: Current measurement techniques and prospects for noninvasive optical methods. *Neurophotonics*, *3*(3), 031411. https://doi.org/10.1117/1.NPh.3.3.031411

Favre, M. E., Lim, V., Falvo, M. J., & Serrador, J. M. (2020). Cerebrovascular reactivity and cerebral autoregulation are improved in the supine posture compared to upright in healthy men and women. *PLOS ONE*, *15*(3), e0229049. https://doi.org/10.1371/journal.pone.0229049

Finucane, C., van Wijnen, V. K., Fan, C. W., Soraghan, C., Byrne, L., Westerhof, B. E., Freeman, R., Fedorowski, A., Harms, M. P. M., Wieling, W., & Kenny, R. (2019). A practical guide to active stand testing and analysis using continuous beat-to-beat non-invasive blood pressure monitoring. *Clinical Autonomic Research*, *29*(4), 427–441. https://doi.org/10.1007/s10286-019-00606-y

Forrester, J. S., Ganz, W., Diamond, G., McHugh, T., Chonette, D. W., & Swan, H. J. C. (1972). Thermodilution cardiac output determination with a single flow-directed catheter. *American Heart Journal*, *83*(3), 306–311. https://doi.org/10.1016/0002-8703(72)90429-2

Freeman, R., Abuzinadah, A. R., Gibbons, C., Jones, P., Miglis, M. G., & Sinn, D. I. (2018). Orthostatic Hypotension. *JACC*, *72*(11), 1294–1309. https://doi.org/10.1016/j.jacc.2018.05.079

Freeman, R., Wieling, W., Axelrod, F. B., Benditt, D. G., Benarroch, E., Biaggioni, I., Cheshire, W. P., Chelimsky, T., Cortelli, P., Gibbons, C. H., Goldstein, D. S., Hainsworth, R., Hilz, M. J., Jacob, G., Kaufmann, H., Jordan, J., Lipsitz, L. A., Levine, B. D., Low, P. A., … Dijk, J. G. (2011). Consensus statement on the definition of orthostatic hypotension, neurally mediated syncope and the postural tachycardia syndrome. *Clinical Autonomic Research*, *21*(2), 69–72. https://doi.org/10.1007/s10286-011-0119-5

Frith, J., Reeve, P., RN, & Newton, J. L. (2013). Length of Time Required to Achieve a Stable Baseline Blood Pressure in the Diagnosis of Orthostatic Hypotension. *Journal of the American Geriatrics Society*, *61*(8), 1414–1415. https://doi.org/10.1111/jgs.12393

Fu, Q., VanGundy, T. B., Galbreath, M. M., Shibata, S., Jain, M., Hastings, J. L., Bhella, P. S., & Levine, B. D. (2010). Cardiac Origins of the Postural Orthostatic Tachycardia Syndrome. *Journal of the American College of Cardiology*, *55*(25), 2858–2868. https://doi.org/10.1016/j.jacc.2010.02.043

Garrett, Z. K., Pearson, J., & Subudhi, A. W. (2017). Postural effects on cerebral blood flow and autoregulation. *Physiological Reports*, *5*(4), e13150. https://doi.org/10.14814/phy2.13150

Geddes, J., Mehlsen, J., & Olufsen, M. S. (2020). Characterization of Blood Pressure and Heart Rate Oscillations of POTS Patients via Uniform Phase Empirical Mode Decomposition. *IEEE Transactions on Biomedical Engineering*, *67*(11), 3016–3025. https://doi.org/10.1109/TBME.2020.2974095

Geerts, B. F., Aarts, L. P., & Jansen, J. R. (2011). Methods in pharmacology: Measurement of cardiac output. *British Journal of Clinical Pharmacology*, *71*(3), 316–330. https://doi.org/10.1111/j.1365-2125.2010.03798.x

Gelinas, J., Marsden, K., Tzeng, Y. C., Smirl, J., Smith, K., Willie, C., Lewis, N., Binsted, G., Bailey, D., Bakker, A., Day, T., & Ainslie, P. (2012). Influence of Posture on the Regulation of Cerebral Perfusion. *Aviation, Space, and Environmental Medicine*, *83*, 751–757. https://doi.org/10.3357/ASEM.3269.2012

Gelpi, F., Bari, V., Cairo, B., De Maria, B., Tonon, D., Rossato, G., Faes, L., & Porta, A. (2021). Correlation Between Baroreflex Sensitivity and Cerebral Autoregulation Index in Healthy Subjects. *2021 Computing in Cardiology (CinC)*, 1–4. https://doi.org/10.23919/CinC53138.2021.9662726

Goodwill, A. G., Dick, G. M., Kiel, A. M., & Tune, J. D. (2017). Regulation of Coronary Blood Flow. *Comprehensive Physiology*, *7*(2), 321–382. https://doi.org/10.1002/cphy.c160016

Gordan, R., Gwathmey, J. K., & Xie, L.-H. (2015). Autonomic and endocrine control of cardiovascular function. *World Journal of Cardiology*, *7*(4), 204–214. https://doi.org/10.4330/wjc.v7.i4.204

Grubb, B. P., Kanjwal, Y., Karabin, B., & Imran, N. (2008). Orthostatic Hypotension and Autonomic Failure: A Concise Guide to Diagnosis and Management. *Clinical Medicine. Cardiology*, *2*, CMC.S926. https://doi.org/10.4137/CMC.S926

Hage, B. D., Truemper, E. J., Bashford, G. R., Hage, B. D., Truemper, E. J., & Bashford, G. R. (2021). Functional Transcranial Doppler Ultrasound for Monitoring Cerebral Blood Flow. *Journal of Visualized Experiments (JoVE)*, (169), e62048. https://doi.org/10.3791/62048

Halliwill, J. R., Taylor, J. A., & Eckberg, D. L. (1996). Impaired sympathetic vascular regulation in humans after acute dynamic exercise. *The Journal of Physiology*, *495 (Pt 1)*(Pt 1), 279–288. https://doi.org/10.1113/jphysiol.1996.sp021592

Hernández, B., Dyer, A. H., McCrory, C., Newman, L., Finucane, C., & Kenny, R. A. (2024). *Which Components of the Haemodynamic Response to Active Stand Predict Cardiovascular Disease and Mortality? Data From The Irish Longitudinal Study on Ageing* (p. 2024.07.30.24311251). medRxiv. https://doi.org/10.1101/2024.07.30.24311251

Hinghofer-Szalkay, H. (2011). Gravity, the hydrostatic indifference concept and the cardiovascular system. *European Journal of Applied Physiology*, *111*(2), 163–174. https://doi.org/10.1007/s00421-010-1646-9

Hussein, S., Renella, R. R., & Dietz, H. (1988). Microsurgical anatomy of the anterior choroidal artery. *Acta Neurochirurgica*, *92*(1), 19–28. https://doi.org/10.1007/BF01401968

Jacob, G., Ertl, A. C., Shannon, J. R., Furlan, R., Robertson, R. M., & Robertson, D. (1998). Effect of standing on neurohumoral responses and plasma volume in healthy subjects. *Journal of Applied Physiology*, *84*(3), 914–921. https://doi.org/10.1152/jappl.1998.84.3.914

Jensen, L. A., Onyskiw, J. E., & Prasad, N. G. N. (1998). Meta-analysis of arterial oxygen saturation monitoring by pulse oximetry in adults. *Heart & Lung: The Journal of Acute and Critical Care*, *27*(6), 387–408. https://doi.org/10.1016/S0147-9563(98)90086-3

Joyner, M. J. (2016). Preclinical and clinical evaluation of autonomic function in humans. *The Journal of Physiology*, *594*(14), 4009–4013. https://doi.org/10.1113/JP271875

Katayama, K., & Ogoh, S. (2025). The role of cardiopulmonary baroreflex on sympathetic vasomotor outflow and blood pressure regulation during dynamic exercise. *Autonomic Neuroscience*, *260*, 103276. https://doi.org/10.1016/j.autneu.2025.103276

Kaufmann, H., Norcliffe-Kaufmann, L., & Palma, J.-A. (2020). Baroreflex Dysfunction. *New England Journal of Medicine*, *382*(2), 163–178. https://doi.org/10.1056/NEJMra1509723

Khan, M. S., Miller, A. J., Ejaz, A., Molinger, J., Goyal, P., MacLeod, D. B., Swavely, A., Wilson, E., Pergola, M., Tandri, H., Mills, C. F., Raj, S. R., & Fudim, M. (2025). Cerebral Blood Flow in Orthostatic Intolerance. *Journal of the American Heart Association*, *14*(3), e036752. https://doi.org/10.1161/JAHA.124.036752

Koep, J. L., Taylor, C. E., Coombes, J. S., Bond, B., Ainslie, P. N., & Bailey, T. G. (2022). Autonomic control of cerebral blood flow: Fundamental comparisons between peripheral and cerebrovascular circulations in humans. *The Journal of Physiology*, *600*(1), 15–39. https://doi.org/10.1113/JP281058

Korner, P. I. (1971). Integrative neural cardiovascular control. *Physiological Reviews*, *51*(2), 312–367. https://doi.org/10.1152/physrev.1971.51.2.312

Kouz, K., Michard, F., Bergholz, A., Vokuhl, C., Briesenick, L., Hoppe, P., Flick, M., Schön, G., & Saugel, B. (2021). Agreement between continuous and intermittent pulmonary artery thermodilution for cardiac output measurement in perioperative and intensive care medicine: A systematic review and meta-analysis. *Critical Care*, *25*(1), 125. https://doi.org/10.1186/s13054-021-03523-7

Kubo, S. H., Burchenal, J. E. B., & Cody, R. J. (1987). Comparison of direct fick and thermodilution cardiac output techniques at high flow rates. *The American Journal of Cardiology*, *59*(4), 384–386. https://doi.org/10.1016/0002-9149(87)90829-0

Lassen, N. A., & Christensen, M. S. (1976). PHYSIOLOGY OF CEREBRAL BLOOD FLOW. *British Journal of Anaesthesia*, *48*(8), 719–734. https://doi.org/10.1093/bja/48.8.719

Levy, M. N. (1979). The cardiac and vascular factors that determine systemic blood flow. *Circulation Research*, *44*(6), 739–747. https://doi.org/10.1161/01.res.44.6.739

Low, P. A., Opfer-Gehrking, T. L., McPhee, B. R., Fealey, R. D., Benarroch, E. E., Willner, C. L., Suarez, G. A., Proper, C. J., Felten, J. A., Huck, C. A., & Corfits, J. L. (1995). Prospective Evaluation of Clinical Characteristics of Orthostatic Hypotension. *Mayo Clinic Proceedings*, *70*(7), 617–622. https://doi.org/10.4065/70.7.617

Macarthur, H., Wilken, G. H., Westfall, T. C., & Kolo, L. L. (2011). Neuronal and non-neuronal modulation of sympathetic neurovascular transmission. *Acta Physiologica*, *203*(1), 37–45. https://doi.org/10.1111/j.1748-1716.2010.02242.x

Mader, S. L., Palmer, R. M., & Rubenstein, L. Z. (1989). Effect of Timing and Number of Baseline Blood Pressure Determinations on Postural Blood Pressure Response. *Journal of the American Geriatrics Society*, *37*(5), 444–446. https://doi.org/10.1111/j.1532-5415.1989.tb02641.x

Malik, M., Bigger, J. T., Camm, A. J., Kleiger, R. E., Malliani, A., Moss, A. J., & Schwartz, P. J. (1996). Heart rate variability: Standards of measurement, physiological interpretation, and clinical use. *European Heart Journal*, *17*(3), 354–381. https://doi.org/10.1093/oxfordjournals.eurheartj.a014868

Mark, A. L., & Mancia, G. (1983). Cardiopulmonary Baroreflexes in Humans. *Comprehensive Physiology*, *1983*(12S8), 795–813. https://doi.org/10.1002/j.2040-4603.1983.tb01001.x

Mathews, L., & Singh, K. R. (2008). Cardiac output monitoring. *Annals of Cardiac Anaesthesia*, *11*(1), 56. https://doi.org/10.4103/0971-9784.38455

Mchedlishvili, G. (1980). Physiological mechanisms controlling cerebral blood flow. *Stroke*, *11*(3), 240–248. https://doi.org/10.1161/01.STR.11.3.240

Meng, L., Hou, W., Chui, J., Han, R., & Gelb, A. W. (2015). Cardiac Output and Cerebral Blood Flow: The Integrated Regulation of Brain Perfusion in Adult Humans. *Anesthesiology*, *123*(5), 1198. https://doi.org/10.1097/ALN.0000000000000872

Milutinović, A., Šuput, D., & Zorc-Pleskovič, R. (2020). Pathogenesis of atherosclerosis in the tunica intima, media, and adventitia of coronary arteries: An updated review. *Bosnian Journal of Basic Medical Sciences*, *20*(1), 21–30. https://doi.org/10.17305/bjbms.2019.4320

Morita, Y., Erik Hardebo, au]Jan, & Bouskela, E. (1994). Influence of cerebrovascular parasympathetic nerves on resting cerebral blood flow, spontaneous vasomotion, autoregulation, hypercapnic vasodilation and sympathetic vasoconstriction. *Journal of the Autonomic Nervous System*, *49*, 9–14. https://doi.org/10.1016/0165-1838(94)90079-5

Mount, C. A., & Das, J. M. (2026). Cerebral Perfusion Pressure. In *StatPearls*. StatPearls Publishing. http://www.ncbi.nlm.nih.gov/books/NBK537271/

Muenter Swift, N., Charkoudian, N., Dotson, R. M., Suarez, G. A., & Low, P. A. (2005). Baroreflex control of muscle sympathetic nerve activity in postural orthostatic tachycardia syndrome. *American Journal of Physiology-Heart and Circulatory Physiology*, *289*(3), H1226–H1233. https://doi.org/10.1152/ajpheart.01243.2004

Munakomi, S., & Das, J. M. (2026). Intracranial Pressure Monitoring. In *StatPearls*. StatPearls Publishing. http://www.ncbi.nlm.nih.gov/books/NBK542298/

Ogoh, S., Brothers, R. M., Barnes, Q., Eubank, W. L., Hawkins, M. N., Purkayastha, S., O-Yurvati, A., & Raven, P. B. (2005). The effect of changes in cardiac output on middle cerebral artery mean blood velocity at rest and during exercise. *The Journal of Physiology*, *569*(Pt 2), 697–704. https://doi.org/10.1113/jphysiol.2005.095836

Olufsen, M. S., Ottesen, J. T., Tran, H. T., Ellwein, L. M., Lipsitz, L. A., & Novak, V. (2005). Blood pressure and blood flow variation during postural change from sitting to standing: Model development and validation. *Journal of Applied Physiology (Bethesda, Md. : 1985)*, *99*(4), 1523–1537. https://doi.org/10.1152/japplphysiol.00177.2005

Pahlavian, S. H., Wang, X., Ma, S., Zheng, H., Casey, M., D'Orazio, L. M., Shao, X., Ringman, J. M., Chui, H., Wang, D. J., & Yan, L. (2021). Cerebroarterial pulsatility and resistivity indices are associated with cognitive impairment and white matter hyperintensity in elderly subjects: A phase-contrast MRI study. *Journal of Cerebral Blood Flow & Metabolism*, *41*(3), 670–683. https://doi.org/10.1177/0271678X20927101

Panerai, R. B., Robinson, T. G., & Minhas, J. S. (2019). The upper frequency limit of dynamic cerebral autoregulation. *The Journal of Physiology*, *597*(24), 5821–5833. https://doi.org/10.1113/JP278710

Parati, G., Di Rienzo, M., Bertinieri, G., Pomidossi, G., Casadei, R., Groppelli, A., Pedotti, A., Zanchetti, A., & Mancia, G. (1988). Evaluation of the baroreceptor-heart rate reflex by 24-hour intra-arterial blood pressure monitoring in humans. *Hypertension*, *12*(2), 214–222. https://doi.org/10.1161/01.HYP.12.2.214

Patel, N. P., Rinaldo, L., & Lanzino, G. (2024). Circle of Willis. *Mayo Clinic Proceedings*, *99*(4), 677–678. https://doi.org/10.1016/j.mayocp.2023.11.020

Peters, A., Schweiger, U., Pellerin, L., Hubold, C., Oltmanns, K. M., Conrad, M., Schultes, B., Born, J., & Fehm, H. L. (2004). The selfish brain: Competition for energy resources. *Neuroscience and Biobehavioral Reviews*, *28*(2), 143–180. https://doi.org/10.1016/j.neubiorev.2004.03.002

Raczak, G., Rovere, M. T. L., Mortara, A., Assandri, J., Prpa, A., Pinna, G. D., Maestri, R., D'Armini, A. M., Viganó, M., & Cobelli, F. (1999). Arterial baroreflex modulation of heart rate in patients early after heart transplantation: Lack of parasympathetic reinnervation. *The Journal of Heart and Lung Transplantation*, *18*(5), 399–406. https://doi.org/10.1016/S1053-2498(98)00071-0

Rajaram, S. S., Desai, N. K., Kalra, A., Gajera, M., Cavanaugh, S. K., Brampton, W., Young, D., Harvey, S., & Rowan, K. (2013). Pulmonary artery catheters for adult patients in intensive care. *The Cochrane Database of Systematic Reviews*, *2013*(2), CD003408. https://doi.org/10.1002/14651858.CD003408.pub3

Reehal, N., Cummings, S., Mullen, M. T., Baker, W. B., Kung, D., Tackett, W., & Favilla, C. G. (2021). Differentiating Dynamic Cerebral Autoregulation Across Vascular Territories. *Frontiers in Neurology*, *12*, 653167. https://doi.org/10.3389/fneur.2021.653167

Reuter, D. A., Huang, C., Edrich, T., Shernan, S. K., & Eltzschig, H. K. (2010). Cardiac Output Monitoring Using Indicator-Dilution Techniques: Basics, Limits, and Perspectives. *Anesthesia & Analgesia*, *110*(3), 799. https://doi.org/10.1213/ANE.0b013e3181cc885a

Robertson, A. D., Edgell, H., & Hughson, R. L. (2014). Assessing cerebrovascular autoregulation from critical closing pressure and resistance area product during upright posture in aging and hypertension. *American Journal of Physiology-Heart and Circulatory Physiology*, *307*(2), H124–H133. https://doi.org/10.1152/ajpheart.00086.2014

Robertson, Andrew., Papadhima, I., & Edgell, H. (2020). Sex differences in the autonomic and cerebrovascular responses to upright tilt. *Autonomic Neuroscience*, *229*, 102742. https://doi.org/10.1016/j.autneu.2020.102742

Robertson, D. (1999, February). *The Epidemic of Orthostatic Tachycardia and Orthostatic Intolerance*. https://oce-ovid-com.ezproxy.library.yorku.ca/article/00000441-199902000-00001/HTML

Robertson, D., Hollister, A. S., Biaggioni, I., Netterville, J. L., Mosqueda-Garcia, R., & Robertson, R. M. (1993). The Diagnosis and Treatment of Baroreflex Failure. *New England Journal of Medicine*, *329*(20), 1449–1455. https://doi.org/10.1056/NEJM199311113292003

Rosner, M. J., & Coley, I. B. (1986). Cerebral perfusion pressure, intracranial pressure, and head elevation. *Journal of Neurosurgery*, *65*(5), 636–641. https://doi.org/10.3171/jns.1986.65.5.0636

Rutkowski, D. R., Barton, G. P., François, C. J., Aggarwal, N., & Roldán-Alzate, A. (2020). Sex Differences in Cardiac Flow Dynamics of Healthy Volunteers. *Radiology: Cardiothoracic Imaging*, *2*(1), e190058. https://doi.org/10.1148/ryct.2020190058

Schurr, J. W., & Genuardi, M. V. (2024). Direct VO2 Measurement: Getting the Fick Right for Heart Transplant Eligibility. *Circulation: Heart Failure*, *17*(1), e011214. https://doi.org/10.1161/CIRCHEARTFAILURE.123.011214

Schwarz, S., Georgiadis, D., Aschoff, A., & Schwab, S. (2002). Effects of Body Position on Intracranial Pressure and Cerebral Perfusion in Patients With Large Hemispheric Stroke. *Stroke*, *33*(2), 497–501. https://doi.org/10.1161/hs0202.102376

Secomb, T. W. (2016). Hemodynamics. *Comprehensive Physiology*, *6*(2), 975–1003. https://doi.org/10.1002/cphy.c150038

Serrador, J. M., & Freeman, R. (2017). Enhanced Cholinergic Activity Improves Cerebral Blood Flow during Orthostatic Stress. *Frontiers in Neurology*, *8*, 103. https://doi.org/10.3389/fneur.2017.00103

Serrador, J. M., Hughson, R. L., Kowalchuk, J. M., Bondar, R. L., & Gelb, A. W. (2006). Cerebral blood flow during orthostasis: Role of arterial CO2. *American Journal of Physiology-Regulatory, Integrative and Comparative Physiology*, *290*(4), R1087–R1093. https://doi.org/10.1152/ajpregu.00446.2005

Serrador, J. M., Picot, P. A., Rutt, B. K., Shoemaker, J. K., & Bondar, R. L. (2000). MRI measures of middle cerebral artery diameter in conscious humans during simulated orthostasis. *Stroke*, *31*(7), 1672–1678. https://doi.org/10.1161/01.str.31.7.1672

Shaffer, F., & Ginsberg, J. P. (2017). An Overview of Heart Rate Variability Metrics and Norms. *Frontiers in Public Health*, *5*, 258. https://doi.org/10.3389/fpubh.2017.00258

Sorond, F. A., Khavari, R., Serrador, J. M., & Lipsitz, L. A. (2005). Regional Cerebral Autoregulation during Orthostatic Stress: Age-Related Differences. *The Journals of Gerontology. Series A, Biological Sciences and Medical Sciences*, *60*(11), 1484–1487. https://doi.org/10.1093/gerona/60.11.1484

St. Pierre, S. R., Peirlinck, M., & Kuhl, E. (2022). Sex Matters: A Comprehensive Comparison of Female and Male Hearts. *Frontiers in Physiology*, *13*, 831179. https://doi.org/10.3389/fphys.2022.831179

Stevens, J. H., Raffin, T. A., Mihm, F. G., Rosenthal, M. H., & Stetz, C. W. (1985). Thermodilution Cardiac Output Measurement: Effects of the Respiratory Cycle on Its Reproducibility. *JAMA*, *253*(15), 2240–2242. https://doi.org/10.1001/jama.1985.03350390082030

Stewart, J. M. (2013). Common Syndromes of Orthostatic Intolerance. *Pediatrics*, *131*(5), 968–980. https://doi.org/10.1542/peds.2012-2610

Thompson, W. O., Thompson, P. K., & Dailey, M. E. (1928). THE EFFECT OF POSTURE UPON THE COMPOSITION AND VOLUME OF THE BLOOD IN MAN. *The Journal of Clinical Investigation*, *5*(4), 573–604. https://doi.org/10.1172/JCI100179

Tiecks, F. P., Lam, A. M., Aaslid, R., & Newell, D. W. (1995). Comparison of Static and Dynamic Cerebral Autoregulation Measurements. *Stroke*, *26*(6), 1014–1019. https://doi.org/10.1161/01.STR.26.6.1014

Tomoto, T., Lu, M., Khan, A. M., Liu, J., Pasha, E. P., Tarumi, T., & Zhang, R. (2023). Cerebral blood flow and cerebrovascular resistance across the adult lifespan: A multimodality approach. *Journal of Cerebral Blood Flow & Metabolism*, *43*(6), 962–976. https://doi.org/10.1177/0271678X231153741

Tse, H.-F., Siu, C.-W., Tsang, V., Yu, C., Park, E., Bornzin, G. A., Benser, M. E., & Lau, C.-P. (2005). Blood Pressure Response to Transition from Supine to Standing Posture Using an Orthostatic Response Algorithm. *Pacing and Clinical Electrophysiology*, *28*(s1), S242–S245. https://doi.org/10.1111/j.1540-8159.2005.00054.x

Tymko, M. M., Ainslie, P. N., & Smith, K. J. (2018). Evaluating the methods used for measuring cerebral blood flow at rest and during exercise in humans. *European Journal of Applied Physiology*, *118*(8), 1527–1538. https://doi.org/10.1007/s00421-018-3887-y

Uchida, Y. (1975). Afferent sympathetic nerve fibers with mechanoreceptors in the right heart. *American Journal of Physiology-Legacy Content*, *228*(1), 223–230. https://doi.org/10.1152/ajplegacy.1975.228.1.223

Valdueza, J. M., Balzer, J. O., Villringer, A., Vogl, T. J., Kutter, R., & Einhäupl, K. M. (1997). Changes in blood flow velocity and diameter of the middle cerebral artery during hyperventilation: Assessment with MR and transcranial Doppler sonography. *AJNR: American Journal of Neuroradiology*, *18*(10), 1929–1934.

van Grondelle, A., Ditchey, R. V., Groves, B. M., Wagner, W. W., & Reeves, J. T. (1983). Thermodilution method overestimates low cardiac output in humans. *American Journal of Physiology-Heart and Circulatory Physiology*, *245*(4), H690–H692. https://doi.org/10.1152/ajpheart.1983.245.4.H690

van Lieshout, J. J., Pott, F., Madsen, P. L., van Goudoever, J., & Secher, N. H. (2001). Muscle Tensing During Standing. *Stroke*, *32*(7), 1546–1551. https://doi.org/10.1161/01.STR.32.7.1546

Vedantam, A., Gopinath, S. P., & Robertson, C. S. (2019). Chapter 1—Acute Management of Traumatic Brain Injury. In *Rehabilitation After Traumatic Brain Injury* (pp. 1–11). Elsevier. https://doi.org/10.1016/B978-0-323-54456-6.00001-3

Vesoulis, Z. A., & Mathur, A. M. (2017). Cerebral Autoregulation, Brain Injury, and the Transitioning Premature Infant. *Frontiers in Pediatrics*, *5*, 64. https://doi.org/10.3389/fped.2017.00064

Vrselja, Z., Brkic, H., Mrdenovic, S., Radic, R., & Curic, G. (2014). Function of Circle of Willis. *Journal of Cerebral Blood Flow & Metabolism*, *34*(4), 578–584. https://doi.org/10.1038/jcbfm.2014.7

Westerhof, B. E., Gisolf, J., Stok, W. J., Wesseling, K. H., & Karemaker, J. M. (2004). Time-domain cross-correlation baroreflex sensitivity: Performance on the EUROBAVAR data

set. *Journal of Hypertension*, *22*(7), 1371–1380. https://doi.org/10.1097/01.hjh.0000125439.28861.ed

Wetzel, R. C., & Latson, T. W. (1985). Major Errors in Thermodilution Cardiac Output Measurement during Rapid Volume Infusion. *Anesthesiology*, *62*(5), 684–687. https://doi.org/10.1097/00000542-198505000-00035

Zarrinkoob, L., Ambarki, K., Wåhlin, A., Birgander, R., Eklund, A., & Malm, J. (2015). Blood flow distribution in cerebral arteries. *Journal of Cerebral Blood Flow and Metabolism: Official Journal of the International Society of Cerebral Blood Flow and Metabolism*, *35*(4), 648–654. https://doi.org/10.1038/jcbfm.2014.241

Zhong, X., Clough, R. H., Panerai, R. B., & Minhas, J. S. (2025). The impact of posture changes on critical closing pressure and resistance-area product regulation in healthy subjects. *European Journal of Applied Physiology*. https://doi.org/10.1007/s00421-025-05972-2